Am J Cancer Res 2023;13(10):4661-4677
www.ajcr.us /ISSN:2156-6976/ajcr0151926

Original Article

Synergistic suppressive effects on triple-negative breast cancer by the combination of JTC-801 and sodium oxamate

Chih-Yang Wang[1,2,3], Do Thi Minh Xuan[1], Pei-Hsuan Ye[4], Chung-Yen Li[5], Gangga Anuraga[2,6], Hoang Dang Khoa Ta[2], Ming-Derg Lai[4,5], Hui-Ping Hsu[7]

[1]Graduate Institute of Cancer Biology and Drug Discovery, College of Medical Science and Technology, Taipei Medical University, Taipei 11031, Taiwan; [2]Ph.D. Program for Cancer Molecular Biology and Drug Discovery, College of Medical Science, Taipei Medical University, Taipei 11031, Taiwan; [3]TMU Research Center of Cancer Translational Medicine, Taipei Medical University, Taipei 11031, Taiwan; [4]Department of Biochemistry and Molecular Biology, College of Medicine, National Cheng Kung University, Tainan 70101, Taiwan; [5]Institute of Basic Medical Sciences, College of Medicine, National Cheng Kung University, Tainan 70101, Taiwan; [6]Department of Statistics, Faculty of Science and Technology, PGRI Adi Buana University, East Java, Surabaya 60234, Indonesia; [7]Department of Surgery, National Cheng Kung University Hospital, College of Medicine, National Cheng Kung University, Tainan 70101, Taiwan

Received June 26, 2023; Accepted September 13, 2023; Epub October 15, 2023; Published October 30, 2023

Abstract: Triple-negative breast cancer (TNBC) poses a significant clinical challenge due to the limited targeted therapies available at present. Cancer cells preferentially use glycolysis as their primary source of energy, characterized by increased glucose uptake and lactate production. JTC-801, a nociception/orphanin FQ opioid peptide (NOP) receptor antagonist, was reported to suppress the opioid receptor-like1 (ORL1) receptor/phosphatidylinositol 3-kinase (PI3K)/protein kinase B (AKT)/nuclear factor (NF)-κB-mediated carbonic anhydrase 9 (CA9) signaling pathway. Sodium oxamate is an inhibitor of gluconeogenesis and a glycolysis inhibitor, as a competitive lactate dehydrogenase A (LDHA) inhibitor, which also produces tumor suppression due to loss of LDHA activity. However, the roles of opioid analgesic drugs (e.g., JTC-801) and glycolysis inhibitors (e.g., sodium oxamate) in TNBC have not fully been explored. Meanwhile, concurrent treatment with JTC-801 and sodium oxamate may cause synergistic anticancer effects in a TNBC model. In the present study, the combination of JTC-801 and sodium oxamate triggered cell death in the TNBC MDA MB-231 cell line. RNA-sequencing data revealed potential genes in the crosstalk between JTC-801 and sodium oxamate including *ALDOC*, *DDIT4*, *DHTKD1*, *EIF6*, *ENO1*, *ENO3*, *FOXK1*, *FOXK2*, *HIF1A*, *MYC*, *PFKM*, *PFKP*, *PPARA,* etc. The combination of JTC-801 and sodium oxamate provides a novel potential therapeutic strategy for TNBC patients via downregulating cell cycle- and amino acid metabolism-related pathways such as "Cell cycle-the metaphase checkpoint", "(L)-tryptophan pathways and transport", and "Glutamic acid pathway". Collectively, the present study demonstrated that the synergistic effect of co-treatment with JTC-801 and sodium oxamate significantly suppressed tumor growth and played a crucial role in tumor development, and in turn may serve as potential synergistic drugs for TNBC.

Keywords: Triple-negative breast cancer, JTC-801, sodium oxamate, glycolysis, cell metabolism, synergistic effect

Introduction

Among the top causes of mortality at the global level, cancers are ranked the second cause of deaths each year which are only surpassed by heart diseases. In 2023, there were an estimated 1.9 million newly diagnosed cancer patients in the United States, and breast cancer patients accounted for more than 20% of that total [1]. In addition, one in three American women with cancer were diagnosed with breast cancer, making it the most prevalent of the female malignancies [2]. In Taiwan, breast cancer is reported to account for 20% of new cancer cases according to the Ministry of Health and Wellness [3]. Breast cancer is categorized into four subtypes according to the immunohistochemical staining of the estrogen receptor (ER), progesterone receptor (PR), human epidermal growth factor receptor-2 (HER-2), and

Ki-67 [4]. Over the last 2 decades, overall survival rates of breast cancer patients improved after the development of targeted agents against hormone receptors or HER-2. In certain countries, the 5-year survival rates currently reach 90%. However, patients with triple-negative breast cancer (TNBC) often develop tumor recurrence, and have a worse 5-year survival rate than those with other subtypes. Despite various advancements in cancer research, treatment of TNBC patients is still a significant clinical challenge. Therefore, developing a novel treatment approach via investigating the carcinogenesis mechanism is critical for TNBC patients.

G protein-coupled receptors (GPCRs) are the largest class of cell surface signaling proteins and are distributed across all cell types. GPCRs are overexpressed in several types of cancer, and activating GPCRs by ligands promotes cell proliferation [5]. Overexpression of protease-activated receptor 1 (PAR1), GPR116, GPR161, and angiotensin II receptor 1 (AGTR1) was reported in breast cancer [6-9]. Opioid-related nociception receptor 1 (OPRL1) is also called nociceptin/orphanin FQ receptor (NOP) and is one of the GPCRs. OPRL1 modulates stress-related disorders [10]; however, several studies suggested that opioid use might promote tumor progression and cause poor survival in advanced cancer patients [11, 12]. OPRL1 expression is higher in cancer patients [13], and methylation of OPRL1 was associated with a methylated group in recurrent oral cancer [14]. N-(4-Amino-2-methyl quinoline-6-yl)-2-(4-ethylphenoxymethyl) benzamide monohydrochloride (JTC-801) was originally identified as a novel antagonist of OPRL1 [15]. Meanwhile, JTC-801 inhibits the proliferation and metastasis of ovarian cancer cells by regulating the phosphatidylinositol 3-kinase (PI3K)-AKT signaling pathway and enhancing apoptosis [16]. JTC-801 also indirectly induces alkaliptosis of cells by inhibiting a pH regulator on the plasma membrane-called carbonic anhydrase 9 (CA9) and the nuclear factor (NF)-κB pathway [17]. However, the significance of OPRL1 and the clinical application of JTC-801 in TNBC have not yet been reported.

Alteration of glucose metabolism is important for cancer cells to adapt to their environment, and lactate dehydrogenase A (LDHA) is a key glycolytic enzyme for converting pyruvate to lactate. LDHA expression is higher in breast cancer tissues than in adjacent tissues and was correlated with a poor prognosis of breast cancer patients. LDHA preserves cancer stemness in TNBC thereby promoting cancer progression [18]. LDHA inhibition suppresses TNBC growth and progression [19]. Sodium oxamate directly inhibits the LDHA-catalyzed conversion process of pyruvate into lactate as a competitive LDHA inhibitor [20]. Sodium oxamate also concomitantly induces apoptosis and autophagy, enhancing the effect against tumor growth and proliferation [21, 22]. However, to the present, due to a lack of high-throughput approaches, the detailed mechanism of sodium oxamate's inhibition of TNBC development is still unclear.

Due to the rapid growth of solid tumors that outstrips neovascularization, a hypoxic microenvironment develops in tumor masses. Cancer cells use anaerobic glycolytic metabolism through LDHA, and lactate accumulates in the tumor microenvironment, resulting in an acidified condition. Therefore, cancer cells express multiple isoforms of carbonic anhydrase to catalyze the hydration of carbon dioxide into bicarbonate and protons. The intracellular pH (pHi) is reversed to counteract acidosis, and CA9 is one of the major prosurvival pHi-regulating enzymes in cancer [23]. CA9 regulates the extracellular pH (pHe) and pHi by catalyzing the reversible hydration of carbon dioxide to carbonic acid to maintain the survival of tumor cells [24]. Combined agents targeting glycolysis or acid-reversing pathways are potential drugs for treating cancer patients.

With this evidence in mind, we hypothesized that due to metabolic pathways and drug-targeting molecules that are aberrantly activated in cancer cells. Therefore, we could attenuate cancer growth by suppressing glycolysis or activating cell death signaling. JTC-801, an antagonist of OPRL1, enhances apoptosis, inhibits CA9, and induces alkaliptosis. Sodium oxamate suppresses glycolysis, and induces apoptosis and autophagy. Combined treatment with JTC-801 and sodium oxamate may have a synergistic effect on cancer treatment. We also performed RNA-sequencing (RNA-Seq) to investigate the mechanism of drug-drug interactions in this study.

Material and methods

Cell culture and real-time quantitative polymerase chain reaction (qPCR)

MDA-MB-231 is a human TNBC cell line, and MCF-7 is an ER-positive breast cancer cell line, both of which were maintained in Dulbecco's modified Eagle medium supplemented with 10% fetal bovine serum, 100 U/ml penicillin, and 100 mg/ml streptomycin under 5% CO_2 at 37°C. RNA from these breast cancer cell line was extracted with the TRIzol reagent (MD Biosciences, Zürich, Switzerland). Next, an iScript™ cDNA Synthesis Kit (Bio-Red, Hercules, CA, USA) was used to generate complementary (c)DNA for the template in a real-time qPCR. Primer sequences were acquired from https://www.origene.com/. cDNA was further analyzed using StepOne™ (Applied Biosystems, Life Technologies, CA, USA) for the qPCRs. The comparative cycle threshold method ($\Delta\Delta C_T$ value) was used to determine messenger (m)RNA levels of each gene, and *GAPDH* was used as a housekeeping gene [25-27].

Western blot analysis

Breast cancer cell were lysed in RIPA buffer containing protease inhibitors. The whole cell lysates were separated using sodium dodecylsulfate polyacrylamide gel electrophoresis (SDS-PAGE), and proteins were transferred onto polyvinylidene difluoride (PVDF) membranes (Millipore, Bedford, MA, USA) using a Hoefer Semiphor Semi-Dry transfer unit (Amersham Pharmacia, San Francisco, CA, USA). The PVDF membranes were incubated with the indicated primary antibody overnight, followed by a secondary peroxidase-conjugated antibody for 1 h [28]. Blots were developed using enhanced chemiluminescence Western blotting detection reagents (Millipore) and detected using a BioSpectrum AC imaging system (UVP, Upland, CA, USA).

3-(4,5-Dimethylthiazol-2-Yl)-2,5-diphenyltetrazolium bromide (MTT) assay

Cell proliferation of transfectants was analyzed by an MTT assay. Cells were seeded into 24-well plates at a density of 2×10^4 cells/well [29]. The MTT reagent was incubated for 4 h, and cell viability was determined at an absorption wavelength of 590 nm [30].

Bioinformatics application in data acquisition and processing

JTC-801 inhibits CA9 [17] and sodium oxamate suppresses LDHA [20]. Expression levels of CA9 and LDHA were evaluated in different cancer cell lines. We obtained normalized mRNA expression data of human cancer cell lines from the Cancer Cell Line Encyclopedia (CCLE) [31]. Gene expressions from 947 cancer cell lines were downloaded and analyzed. Downregulated genes in JTC-801- and sodium oxamate-treated MDA-MB-231 cells were explored, and the prognostic values of these genes were examined with the Kaplan-Meier plotter (KM Plot) database. A Kaplan-Meier (KM) survival curve, log-rank *p* values, and hazard ratios (HRs) with 95% confidence intervals (CIs) were calculated according to default settings [32].

RNA-Seq and data processing

The RNA of each sample was extracted using the TRIzol® reagent (ThermoFisher Scientific, Madison, WI, USA). The RNA quality, RNA-Seq, sequencing quality trimming, and mRNA alignment were carried out by Genomics BioSci and Technology (Taipei, Taiwan). Briefly, raw data were further mapped onto Ensembl features using packages attached to the biomaRt tool (vers. 2.26.1), and the CLC Genomics Workbench (vers. 10.1, CLC bio, Aarhus, Denmark) was utilized to examine the data and gene symbols. Signals were subsequently processed and standardized, as mentioned earlier, to visualize results as a clustered heatmap based on mRNA expression patterns (vers. 1.0.12) of one of the CRAN packages supported by the R environment [33-35], as well as an online platform (http://www.bioinformatics.com.cn/srplot). For the subsequent discovery of groups of enriched functionally related genes, the Database for Annotation, Visualization, and Integrated Discovery (DAVID) [36, 37], and the Gene Ontology (GO) and Kyoto Encyclopedia of Genes and Genomes (KEGG) platform were used as previously described [38, 39]. The top 5% of up- or downregulated genes derived from the JTC-801 and sodium oxamate groups were further processed by GO analyses [40], while $P < 0.05$ and an adjusted false discovery rate (FDR) of 0.05 were set as the significance levels [41]. The Enrichment Analysis Workflow and GeneGO analysis network from MetaCore (St. Joseph, MN, USA) were designed to identify biological

processes (BPs) related to gene expression data [42]. The top 5% of up- or downregulated genes with substantial differences in transcriptome levels were processed into MetaCore, and we compared average levels of gene expressions in both models. A statistically significant difference was indicated by $P < 0.05$ [43, 44].

Statistical analysis

All statistical analyses were conducted using GraphPad Prism (GraphPad Software, San Diego, CA, USA). These analyses were performed using an unpaired Student's *t*-test or one-way analysis of variance (ANOVA) to analyze differences between experimental groups [45-47].

Results

Expressions of JTC-801-induced key genes in different types of breast cancer

Since CA9 is a target protein of JTC-801, we examined CA9 expression in the CCLE database. High CA9 expression was observed in TNBC cell lines, including MDA-MB-231, Hs-578t, and MDA-MB-468 cells (Supplementary Figure 1A). Increased expressions of CA9 were also observed in TNBC breast cancer patients from the TGCA database (Supplementary Figure 1B). We further validated these data with a Western blot analysis, and results were consistent with RNA-Seq data from the CCLE database. Significantly increased CA9 expression was detected in TNBC MDA-MB-231 cells compared to ER-positive (ER^+) MCF-7 cells (Supplementary Figure 1C). High CA9 mRNA expression was correlated with poor disease-free survival of most types of breast cancer patients in the KM Plot, especially those with basal-type breast cancer (Supplementary Figure 1D).

Expressions of key sodium oxamate-induced genes in different types of breast cancer

Because LDHA is a target protein of sodium oxamate, we examined LDHA expression in the CCLE database. High LDHA expressions were observed in TNBC cell lines, including MDA-MB-231, Hs578t, and MDA-MB-468 cells (Supplementary Figure 2A). Increased LDHA expressions were also observed in TNBC breast cancer patients from TGCA database (Supplementary Figure 2B). We also validated these data with a Western blot analysis, and results were consistent with RNA-Seq data from the CCLE database. Significantly increased expression of LDHA was detected in TNBC MDA-MB-231 cells compared to ER^+ MCF-7 cells (Supplementary Figure 2C). High LDHA mRNA expression was correlated with poor survival of most types of breast cancer patients in the Kaplan-Meier Plotter (Supplementary Figure 2D).

Combination therapy with JTC-801 and sodium oxamate in breast cancer

TNBC MDA-MB-231 and ER^+ MCF-7 cells were treated with JTC-801 or sodium oxamate, and cell viability was measured by an MTT assay. MDA-MB-231 cells were more sensitive to JTC-801 (**Figure 1A**). However, both cell lines exhibited a similar response to sodium oxamate (**Figure 1B**). The synergistic effect of these two drugs was also evaluated by treatment with JTC-801 (2.5 μM), sodium oxamate (10 mM), and their combination (2.5 μM JTC-801 plus 10 mM sodium oxamate). An additive therapeutic effect was observed in the combination group of MDA-MB-231 cells (**Figure 1C**). Our results suggested that expressions of JTC-801-regulated genes differed in MDA MB-231 cells, which may express higher levels of the target protein. Because of higher levels of LDHA and CA9 in MDA-MB-231 cells (Supplementary Figures 1A, 2A). However, MDA-MB-231 cells were deemed more sensitive to combination therapy. Therefore, we chose MDA-MB-231 cells for further experiments.

Differentially increased genes and GO analysis of MDA-MB-231 cells cotreated with JTC-801 and sodium oxamate

According to RNA-Seq data, we used GO enrichment to analyze potential BPs in JTC-801-treated, sodium oxamate-treated, and JTC-801/sodium oxamate-cotreated MDA-MB-231 cells. In comparisons of gene expression patterns, GO pathways that had increased in the control group were categorized as cluster 1, and included "viral transcription (GO:0019083)", "nuclear-transcribed mRNA catabolic process, nonsense-mediated decay (GO:0000184)", "translational initiation (GO:0006413)", "SRP-dependent cotranslational protein targeting to

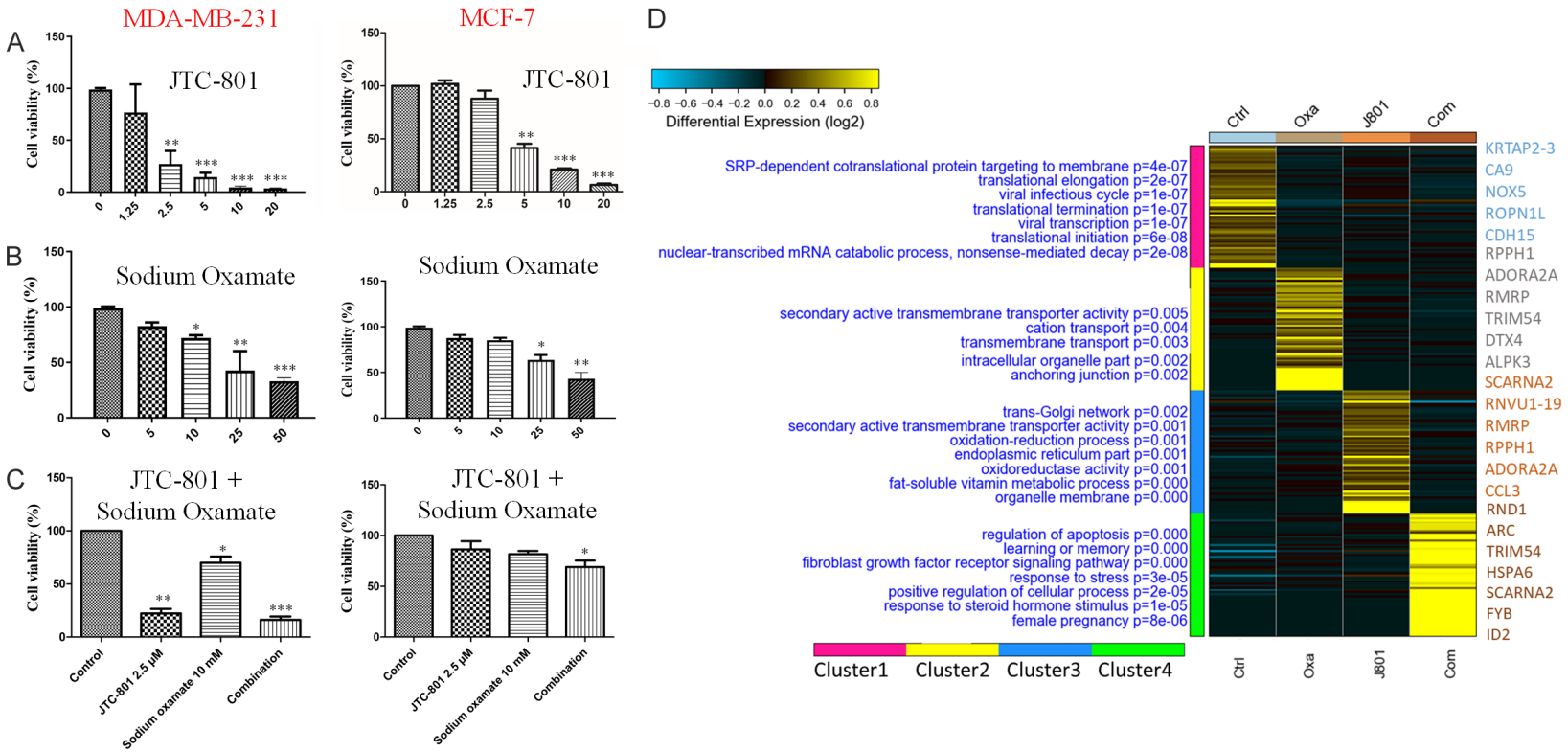

Figure 1. Cell proliferation evaluated by an MTT assay and analytical results of gene ontology (GO) enrichment accompanied with heatmap visualization in the group cotreated with sodium oxamate and JTC-801. (A) Viability of MDA-MB-231 and MCF-7 cells after treatment with different concentrations of JTC-801 (an opioid analgesic drug) and (B) sodium oxamate (a glycolysis inhibitor). (C) Treatment with JTC-801 and sodium oxamate. The combined effects of an opioid analgesic drug and glycolysis inhibitor were investigated. Cell viability was measured after treatment for 48 h. (D) Comparison of gene expression patterns between control (Ctrl), opioid analgesic drug (JTC-801)-treated, sodium oxamate (Oxa)-treated, and JTC-801/sodium oxamate-cotreated (com) MDA-MB-231 cells as well as a control group. Cluster 1 is the control group that contained the most significantly increased pathways compared to other groups, cluster 2 contains those in the sodium oxamate-treated group, cluster 3 contains those in the JTC-801-treated group, and cluster 4 contains pathways in the cotreated group.

membrane (GO:0006614)", and "RNA splicing (GO:0008380)" (**Figure 1D**). Upregulated genes in the control group included *KRTAP2-3*, *CA9*, *NOX5*, *ROPN1L*, and *CDH15*.

Cluster 2 included BPs with increased expression in the oxamate-treated group compared to other groups included "anchoring junction (GO:0070161)", "intracellular organelle part (GO:0044446)", "secondary active transmembrane transporter activity", "cation transport", and "transmembrane transport" (**Figure 1D**). Upregulated genes in the oxamate-treated group included *RPPH1*, *ADORA2A*, *RMRP*, *TRIM54*, *DTX4*, and *ALPK3*.

Cluster 3 were GO pathways upregulated in the JTC-801-treated group compared to other groups, containing "fat-soluble vitamin metabolic process (GO:0006775)", "oxidoreductase activity (GO:0016491)", "endoplasmic reticulum part (GO:0044432)", "secondary active transmembrane transporter activity (GO:0015291)", "monocarboxylic acid metabolic process (GO:0032787)", and "regulation of ERK1 and ERK2 cascades (GO:0070372)" (**Figure 1D**). Upregulated genes in the JTC-801-treated group included *SCARNA2*, *RNVU1-19*, *RMRP*, *RPPH1*, *ADORA2A*, and *CCL3*.

Cluster 4 consisted of highly expressed GO pathways in the group cotreated with JTC-801 and sodium oxamate, such as "response to steroid hormone stimulus (GO:0048545)", "response to stress (GO:0006950)", "fibroblast growth factor receptor signaling pathway (GO:0008543)", "learning or memory (GO:0007611)", "BMP signaling pathway (GO:0030509)", and "regulation of cell proliferation (GO:0042127)" (**Figure 1D**). Upregulated genes in the group cotreated with JTC-801 and sodium oxamate included *RND1*, *ARC*, *TRIM54*, *HSPA6*, *SCARNA2*, *FYB*, and *ID2*.

Downregulated pathways in JTC-801- or sodium oxamate-treated MDA MB-231 cells

From RNA-Seq data of JTC-801-treated MDA MB-231 cells compared to the control group, the top 5% up- or downregulated gene expressions were uploaded to the MetaCore database for a pathway analysis. Downregulated pathways in JTC-801-treated cells included "Protein folding and maturation_Angiotensin system maturation", "Cell adhesion_Classical cadherin-mediated cell adhesion", "G-protein signaling_RhoA activation", "Signal transduction_WNT/Beta-catenin signaling in tissue homeostasis", and "Cell adhesion_Tight junctions" (**Figure 2A**, Supplementary Figure 3A; Supplementary Table 1). Downregulated pathways in sodium oxamate-treated cells included "Apoptosis and survival_Granzyme A signaling", "Muscle contraction_GPCRs in the regulation of smooth muscle tone", "Development_Androgen receptor in the reproductive system", "Cytoskeleton remodeling_Alpha-1A adrenergic receptor-dependent inhibition of PI3K", and "Development_NOTCH signaling in organogenesis and embryogenesis" (**Figure 2B**, Supplementary Figure 4A; Supplementary Table 2). Downregulated pathways in JTC-801/sodium oxamate-cotreated cells included "Cell cycle_The metaphase checkpoint", "Cell cycle_Chromosome condensation in prometaphase", "Cell cycle_Spindle assembly and chromosome separation", "Cell cycle_Role of APC in cell cycle regulation", "Cell cycle_Role of Nek in cell cycle regulation", and "DNA damage_ATM/ATR regulation of G2/M checkpoint: nuclear signaling" (**Figure 2C**, Supplementary Figure 5A; Supplementary Table 3).

Upregulated pathways in JTC-801- or sodium oxamate-treated MDA MB-231 cells

We used a similar approach as mentioned above to analyze RNA-Seq data from sodium oxamate-treated MDA-MB-231 cells. Several upregulated maps were found in JTC-801-treated cells, including "IL-1 signaling in melanoma", "Immune response_IL-17 signaling pathways", "TNF-alpha and IL-1 beta-mediated regulation of contraction and secretion of inflammatory factors", "Release of proinflammatory mediators and elastolytic enzymes by alveolar macrophages", and "NF-κB-, AP-1- and MAPKs-mediated proinflammatory cytokine production" (**Figure 3A**, Supplementary Figure 3B; Supplementary Table 4). We used a similar approach as mentioned above to analyze RNA-Seq data from sodium oxamate-treated MDA-MB-231 cells. Several upregulated maps were found in sodium oxamate-treated cells, including "COVID-19-associated coagulopathy", "Aminoglycoside- and cisplatin-induced hair cell death", "Transport_HDL-mediated reverse cholesterol transport", "Immune response histamine H1 receptor signaling in immune response", and "Glucocorticoids-mediated inhibition of pro-constrictory and proinflammatory

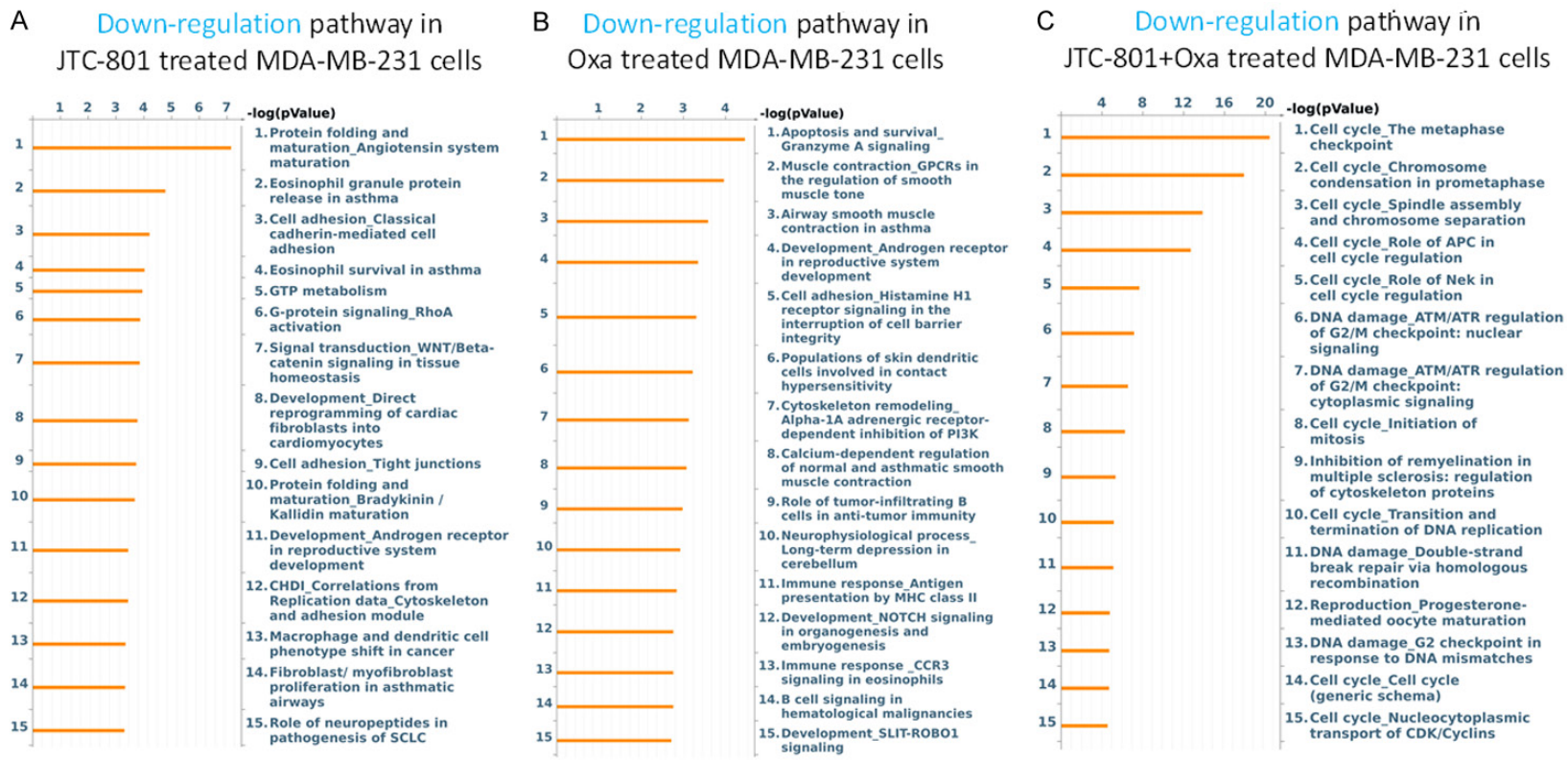

Figure 2. MetaCore pathway analysis of downregulated pathways in JTC-801-treated, sodium oxamate-treated, and cotreated MDA-MB-231 cells. (A) MetaCore pathway analysis of JTC-801-treated MDA-MB-231 cells, (B) Sodium oxamate-treated cells, and (C) JTC-801/sodium oxamate-cotreated cells. The left panel presents downregulated pathways, whereas the right panel presents upregulated pathways.

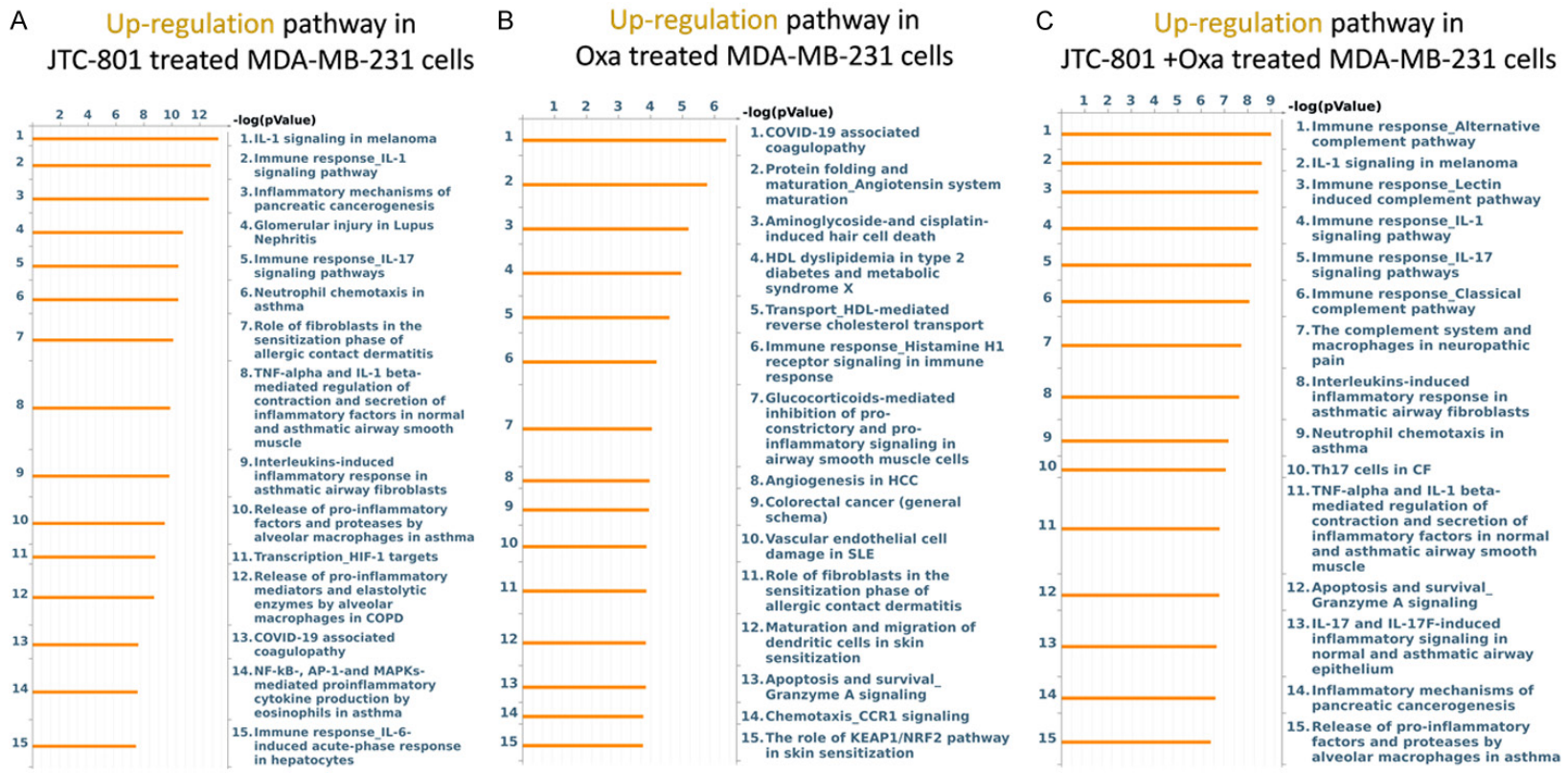

Figure 3. MetaCore pathway analysis of upregulated pathways in JTC-801-treated, sodium oxamate-treated, and cotreated MDA-MB-231 cells. (A) MetaCore pathway analysis of JTC-801-treated MDA-MB-231 cells, (B) Sodium oxamate-treated cells, and (C) JTC-801/sodium oxamate-cotreated cells. The left panel presents down-regulated pathways, whereas the right panel presents upregulated pathways.

signaling" (**Figure 3B**, Supplementary Figure 4B; Supplementary Table 5). We also analyzed RNA-Seq data from JTC-801/sodium oxamate-cotreated MDA-MB-231 cells. Several upregulated maps were found, including "Immune response_Alternative complement pathway", "IL-1 signaling in melanoma", "Immune response_Lectin-induced complement pathway", "Immune response_IL-17 signaling pathways", and "Interleukins-induced inflammatory response in asthmatic airway fibroblasts" (**Figure 3C**, Supplementary Figure 5B; Supplementary Table 6).

Downregulation of glycolysis- and amino acid metabolism-related pathways in JTC-801/sodium oxamate-cotreated MDA-MB-231 cells

We used a bioinformatics approach to identify potential pathways associated with low-expressed genes in JTC-801/sodium oxamate-cotreated MDA-MB-231 cells. Endogenous networks of metabolic-related pathways were analyzed using the MetaCore platform. A Venn diagram presents down-expressed pathways in JTC-801/sodium oxamate-cotreated cells (**Figure 4A**). The 495 intersecting genes from the above diagram were further uploaded to the MetaCore platform for a Metabolic Networks (Endogenous) analysis. Downstream pathway analyses revealed that glycolysis- and amino acid-related metabolic pathways were significantly correlated with JTC-801-/sodium oxamate-cotreated MDA-MB-231 cells, including "(L)-tryptophan pathways and transport", "Glutamic acid pathway", "(L)-proline pathways and transport", "L-glutamate pathways and transport", "Glycine pathway", "(L)-valine pathways and transport", and "Amino acid metabolism_Asparagine, Aspartic acid metabolism and transport", and most of these downstream molecules in the above metabolic pathways may either directly or indirectly regulate glycolysis in JTC-801/sodium oxamate-cotreated MDA-MB-231 cells (**Figure 4B**). (C) Downstream pathway analyses based on these top lower-expressing genes revealed that the "L-glutamate pathways and transport" pathway was significantly correlated with JTC-801/sodium oxamate-cotreated MDA-MB-231 cells (**Figure 4C**).

Correlations between the survival of breast cancer patients and JTC-801 and sodium oxamate downregulated glycolysis-related genes

Next, we investigated correlations between downregulated glycolysis-related genes in the JTC-801/sodium oxamate-cotreated group and the status of breast cancer patients. First, glycolysis-related genes were found via Gene Ontology Terms (GO:0006096)-glycolytic process [48]. Expression levels of 95 glycolysis-related genes were correlated with clinical outcomes of 1764 breast cancer patients in the KM Plot database. Several glycolysis-related genes were correlated with poor prognoses of breast cancer patients, including *ALDOC* (aldolase C, fructose-bisphosphate), *BPGM* (2,3-bisphosphoglycerate mutase), *DDIT4* (DNA damage inducible transcript 4), *DHTKD1* (dehydrogenase E1 and transketolase domain containing 1), *EIF6* (eukaryotic translation initiation factor 6), *ENO1* (enolase 1), *ENO3* (enolase 3), *FOXK1* (forkhead box K1), *FOXK2* (forkhead box K2), *GALT* (galactose-1-phosphate uridylyl transferase), *GAPDH* (glyceraldehyde-3-phosphate dehydrogenase), *GIT1* (G protein-coupled receptor kinase interacting ArfGAP 1), *HIF1A* (hypoxia inducible factor 1, alpha subunit), *MYC* (v-Myc avian myelocytomatosis viral oncogene homolog), *PFKFB2* (6-phosphofructo-2-kinase/fructose-2,6-biphosphatase 2), *PFKL* (phosphofructokinase, liver), *PFKM* (phosphofructokinase, muscle), *PFKP* (phosphofructokinase, platelet), *PGAM1* (phosphoglycerate mutase 1), *PGK1* (phosphoglycerate kinase 1), *PPARA* (peroxisome proliferator-activated receptor alpha), *PPARGC1A* (peroxisome proliferator-activated receptor gamma, coactivator 1 alpha), *SLC2A9* (solute carrier family 2, member 9), *TIGAR* (TP53 induced glycolysis regulatory phosphatase), and *TPI1* (triosephosphate isomerase 1) (**Figure 5**). We examined OPRL1 expression in breast cancer cell lines in CCLE and level of OPRL1 was slightly lower in MDA-MB-231 cells (Supplementary Figure 6A). We further studied opioid receptor- and glycolysis-related genes in MDA-MB-231 cells by a qPCR and expressions of these genes decreased after combined treatment with JTC-801 and sodium oxamate (Supplementary Figure 6B and 6C).

Correlations between the survival of breast cancer patients and JTC-801 and sodium oxamate downregulated genes

In order to explore downstream molecules other than those related to the glycolysis pathway, we investigated the most strongly downregulated genes in the cotreated group, and expressions of target genes were correlated with the survival status of breast cancer

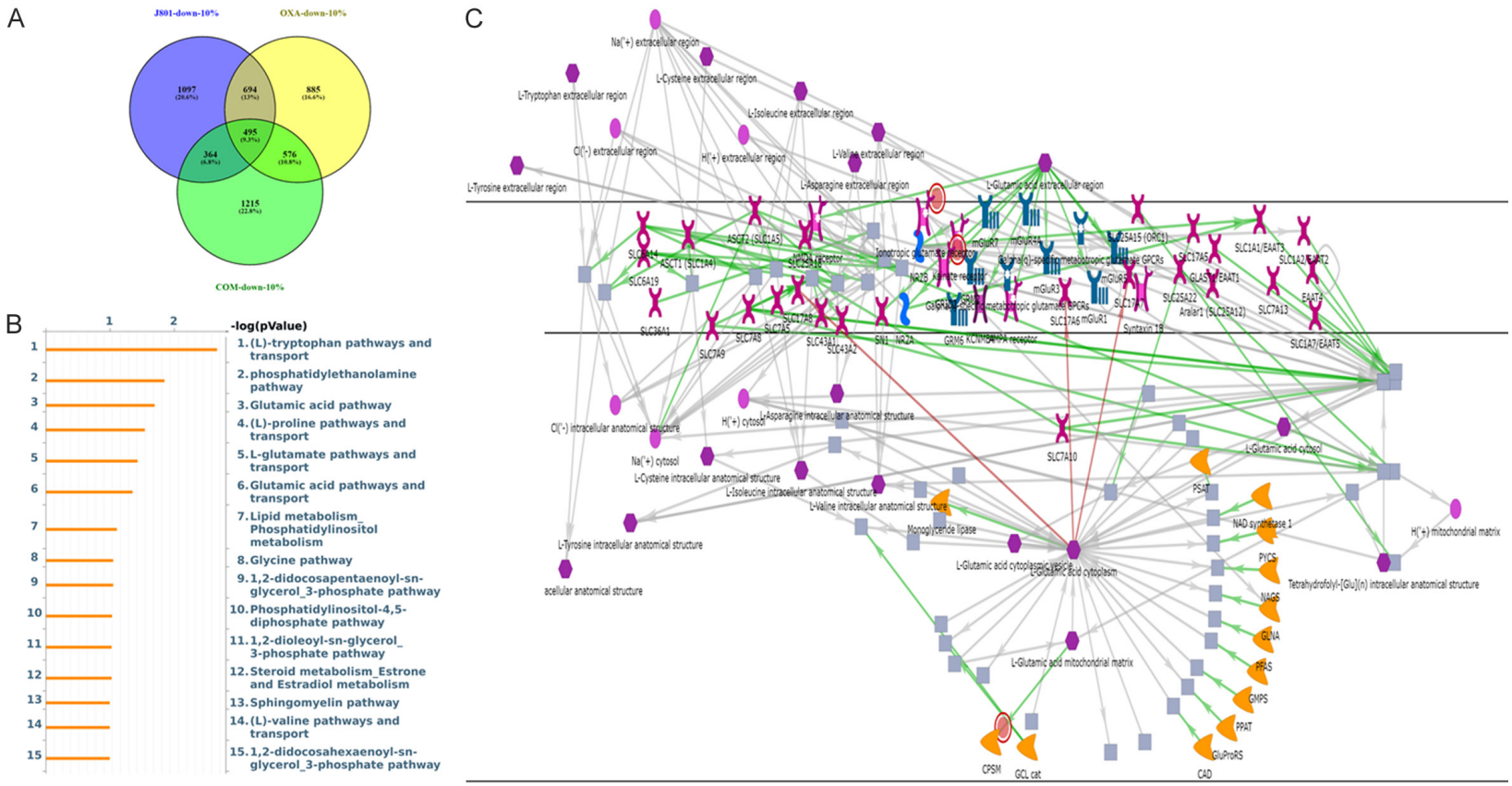

Figure 4. Endogenous Metabolic Networks analysis of metabolism-related pathways in JTC-801/sodium oxamate-cotreated MDA-MB-231 cells via the MetaCore platform. A. Venn diagram of down-expressed pathways and networks in JTC-801/sodium oxamate-cotreated cells. The blue circle represents 10% down-expressed genes in JTC-801-treated MDA-MB-231 cells, the yellow circle represents 10% down-expressed genes in the sodium oxamate-treated group, and the green circle represents 10% down-expressed genes in the JTC-801/sodium oxamate-cotreated group. B. The 495 intersecting genes from the above circles were uploaded to the MetaCore platform for analysis of endogenous metabolic networks. Glycolysis- and amino acid-related metabolic pathways were significantly increased in JTC-801/sodium oxamate-cotreated MDA-MB-231 cells. C. "L-glutamate pathways and transport" was significantly correlated with low-expressed genes in JTC-801/sodium oxamate-cotreated MDA-MB-231 cells.

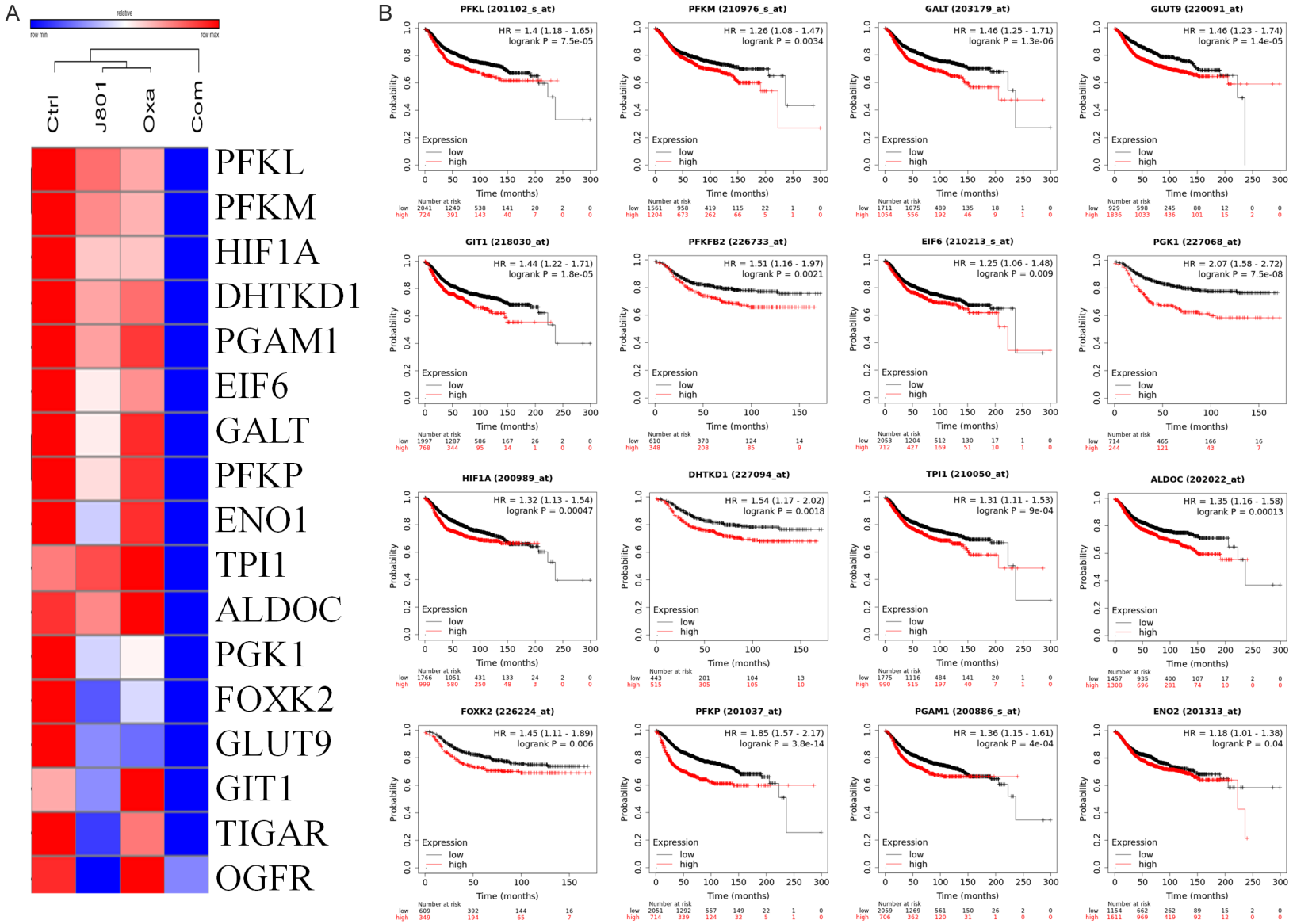

Figure 5. Relationships between glycolysis- and opioid receptor-related genes in the JTC-801/sodium oxamate-cotreated group and distant metastasis-free survival in breast cancer patients. A. A heatmap represents glycolysis-related genes in the JTC-801/sodium oxamate-cotreated group via RNA-Seq data of MDA-MB-231 cells. B. The impacts of the above genes on the survival status of breast cancer patients were studied using the KM Plot database. Red lines indicate high transcriptional expression levels, and black lines represent low expression levels.

patients in the KM Plot database. High mRNA expression levels of several genes were correlated with poor survival of breast cancer patients, including *CA9*, *CAV3* (caveolin 3), *CCNB2* (cyclin B2), *CDCA3* (cell division cycle associated 3), *CDH15* (cadherin 15), *CDKN3* (cyclin-dependent kinase inhibitor 3), *CTSE* (cathepsin E), *DLGAP5* (discs large homolog associated protein 5), *GPRC5C* (G protein-coupled receptor, class C, group 5, member C), *HRCT1* (histidine rich carboxyl terminus 1), *KIF20A* (kinesin family member 20A), *LMO3* (LIM domain only 3 (rhombotin-like 2), *MAP2K6* (mitogen-activated protein kinase kinase 6), *MUC5B* (mucin 5B, oligomeric mucus/gel-forming), *MYBPH* (myosin-binding protein H), *PAPPA2* (pappalysin 2), *STK31* (serine/threonine kinase 31), *TAS2R14* (taste receptor, type 2, member 14), and *TCP11* (t-complex 11, testis-specific). Since these genes significantly decreased after cotreatment with JTC-801 and sodium oxamate, they may play important roles in regulating cell death during TNBC development (Supplementary Figure 7).

Discussion

Patients with TNBC have higher risks of recurrence and a worse survival chance than those with other subtypes. From our study, we found that higher expressions of the intracellular pH-regulating protein, CA9, and glucose metabolism protein, LDHA, were detected in tumor specimens and cancer cell lines from TNBC patients. The OPRL1 antagonist, JTC-801, suppresses CA9 expression and induces cell death. Sodium oxamate inhibits LDHA and restrains cell proliferation. Cell cycle- and metabolism-related pathways were downregulated, and immune-activated pathways were upregulated in cells simultaneously treated with both drugs. Combined treatment with JTC-801 and sodium oxamate is a potential therapeutic strategy for TNBC patients. In our study, agents targeting opioid-related and glycolysis pathways had synergistic effects in cancer therapy.

The Warburg effect, first described by Otto Warburg, is a metabolic phenotype that allows tumor tissues to enhance the uptake and conversion of glucose anaerobically (glycolysis) rather than aerobically (mitochondrial oxidative phosphorylation), even in the presence of adequate oxygen. TNBC cells express higher LDHA levels but lower oxygen consumption rates compared to luminal breast cancer cells [49]. In addition, key molecules in the glycolytic pathways, including glucose transporter 1, hexokinase 2, pyruvate kinase 2 isoenzyme, and LDHA, are all highly expressed in TNBC to support active glycolysis pathways [50]. The glycolytic generation of lactate is an important part of extracellular acidification [51, 52]. Sodium oxamate inhibits LDHA-catalyzed conversion of pyruvate into lactate [20]. The combination of doxorubicin, metformin, and oxamate resulted in efficient and rapid tumor growth inhibition in a breast cancer model [53]. The combined approach of an indirect HIF-1α inhibitor, menadione, and a glycolysis inhibitor, sodium oxamate, may be a promising treatment strategy for colon cancer [54]. In our study, we confirmed that treatment with sodium oxamate suppressed proliferation of TNBC cancer cells.

Since aerobic glycolysis is the predominant metabolic mode of cancer cells, the increased fermentation of glucose to lactate leads to extracellular acidification. The direct qualitative measurement of the glycolytic rate represents the level of extracellular acidification. The pHi of differentiated adult cells is maintained at around 7.2, while the pHe is around 7.4. The balance of pHe and pHi in most cancer cells differs greatly from that of normal cells, and the pHe is lower (6.7~7.1) inside the cancer mass [55, 56]. In general, the pHi of cancer cells seems to be more uniform than the pHe. pHi values are distributed across quite a narrow range compared to the pHe. While glucose remains electrically neutral at physiological pH (approximately 7), lactate accumulation (pKa 3.86) in cancer cells contributes to the low pHi, since it mainly exists in the carboxylate anion form [57]. Cancer cells express multiple isoforms of carbonic anhydrase to catalyze the hydration of carbon dioxide into bicarbonate and protons for counteracting acidosis, and reversing pHi. CA9 is one of the major prosurvival pHi-regulating enzymes in cancer [23]. The OPRL1 antagonist, JTC-801, also indirectly induces alkaliptosis in cells by inhibiting CA9 in plasma membranes and the cytoplasmic NF-κB pathway [17]. Meanwhile, we also examined the OPRL1 expression in breast cancer cell lines and validated bioinformatics data in MDA-MB-231 cells (Supplementary Figure 7).

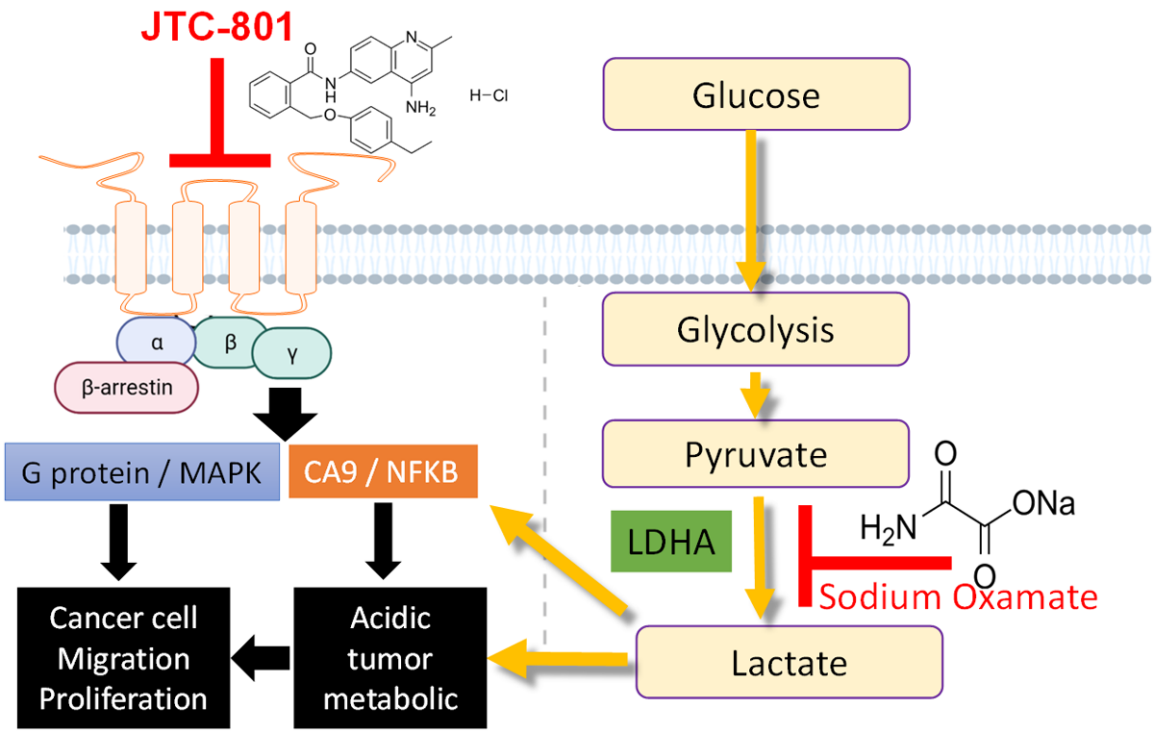

Figure 6. Schematic diagram of an effective cancer suppression process through combination therapy of JTC-801 plus sodium oxamate.

Numerous cytotoxic drugs, including alkaloids, anthraquinones, alkylating compounds, and antimetabolites, have been combined to treat breast cancer. Recurrence and metastases due to multidrug resistance are still huge challenges for oncologists. Developing new combined regimens is currently important. Targeting glycolysis and pHi-regulating pathways is a reasonable synergistic combination. Therefore, we cotreated TNBC cell lines with JTC-801 and sodium oxamate and confirmed a synergistic effect. In addition, one of the most prominent characteristics of cancer is dysregulation of the cell cycle involving metabolic abnormalities. JTC-801 causes apoptosis of cancer cells through PI3K/AKT signaling [16]. Sodium oxamate also induces apoptosis against tumor growth and proliferation [21, 22]. Our data were consistent with previous research. The RNA-Seq data revealed that several potential pathways were involved in the cooperative cytotoxic effect of JTC-801 and sodium oxamate, especially those associated with the cell cycle and DNA damage repair.

We also found that JTC-801 regulated inflammatory and homeostasis-related pathways. High mRNA expression levels of several genes were correlated with poor prognoses of breast cancer patients, including *ALDOC*, *BPGM*, *DDIT4*, *DHTKD1*, *EIF6*, *ENO1*, *ENO3*, *FOXK1*, *FOXK2*, *GALT*, *GIT1*, *HIF1A*, *MYC*, *PFKFB2*, *PFKL*, *PFKM*, *PFKP*, *PGAM1*, *PGK1*, *PPARA*, *PPARGC1A*, *SLC2A9*, *TIGAR*, and *TPI1*. The combination of JTC-801 and sodium oxamate upregulated immune-related pathways and suppressed metabolism-related ones. From our results, cotreatment with these two drugs provided a novel potential therapeutic regimen for TNBC patients.

In conclusion, our present study demonstrated that co-treatment with JTC-801 and sodium oxamate significantly suppressed tumor growth and played a crucial role in tumor development, which in term may serve as potential synergistic drugs for TNBC (**Figure 6**).

Acknowledgements

This research was supported by grants from the Ministry of Science and Technology of Taiwan (MOST 110-2314-B-006-087 to MD Lai, 109-2314-B-006-018-MY3 to H.P.H., and

109-2320-B-038-009-MY2 and 112-2320-B-038-024 to C.Y.W.), the National Cheng Kung University Hospital (grant nos. NCKUH-10902031 and NCKUH-11002013 to H.P.H.), and the TMU Research Center of Cancer Translational Medicine from The Featured Areas Research Center Program within the framework of the Higher Education Sprout Project by the Ministry of Education (MOE) in Taiwan. The authors acknowledge the online platform for data analysis and visualization (http://www.bioinformatics.com.cn/). The authors truly appreciate Mr. Daniel P. Chamberlin from the Office of Research and Development at Taipei Medical University for professional English editing. The authors acknowledge the statistical/computational/technical support of the Clinical Data Center, Office of Data Science, Taipei Medical University, Taiwan.

Disclosure of conflict of interest

None.

Address correspondence to: Hui-Ping Hsu, Department of Surgery, National Cheng Kung University Hospital, College of Medicine, National Cheng Kung University, Tainan 70101, Taiwan. Tel: +886-6-2353535 Ext. 5272; E-mail: hphsu@mail.ncku.edu.tw

References

[1] Siegel RL, Miller KD, Wagle NS and Jemal A. Cancer statistics, 2023. CA Cancer J Clin 2023; 73: 17-48.

[2] Lei S, Zheng R, Zhang S, Wang S, Chen R, Sun K, Zeng H, Zhou J and Wei W. Global patterns of breast cancer incidence and mortality: a population-based cancer registry data analysis from 2000 to 2020. Cancer Commun (Lond) 2021; 41: 1183-1194.

[3] Su SY. Nationwide mammographic screening and breast cancer mortality in Taiwan: an interrupted time-series analysis. Breast Cancer 2022; 29: 336-342.

[4] Lin CW and Chang CC. Breast Cancer Detection Using Surface Plasmon Resonance-Based Biosensors. 2011. pp. 17.

[5] Singh A, Nunes JJ and Ateeq B. Role and therapeutic potential of G-protein coupled receptors in breast cancer progression and metastases. Eur J Pharmacol 2015; 763: 178-183.

[6] Hernández NA, Correa E, Avila EP, Vela TA and Pérez VM. PAR1 is selectively over expressed in high grade breast cancer patients: a cohort study. J Transl Med 2009; 7: 47.

[7] Tang X, Jin R, Qu G, Wang X, Li Z, Yuan Z, Zhao C, Siwko S, Shi T, Wang P, Xiao J, Liu M and Luo J. GPR116, an adhesion G-protein-coupled receptor, promotes breast cancer metastasis via the Gαq-p63RhoGEF-Rho GTPase pathway. Cancer Res 2013; 73: 6206-6218.

[8] Feigin ME, Xue B, Hammell MC and Muthuswamy SK. G-protein-coupled receptor GPR161 is overexpressed in breast cancer and is a promoter of cell proliferation and invasion. Proc Natl Acad Sci U S A 2014; 111: 4191-4196.

[9] Rhodes DR, Ateeq B, Cao Q, Tomlins SA, Mehra R, Laxman B, Kalyana-Sundaram S, Lonigro RJ, Helgeson BE, Bhojani MS, Rehemtulla A, Kleer CG, Hayes DF, Lucas PC, Varambally S and Chinnaiyan AM. AGTR1 overexpression defines a subset of breast cancer and confers sensitivity to losartan, an AGTR1 antagonist. Proc Natl Acad Sci U S A 2009; 106: 10284-10289.

[10] Ubaldi M, Cannella N, Borruto AM, Petrella M, Micioni Di Bonaventura MV, Soverchia L, Stopponi S, Weiss F, Cifani C and Ciccocioppo R. Role of nociceptin/orphanin FQ-NOP receptor system in the regulation of stress-related disorders. Int J Mol Sci 2021; 22: 12956.

[11] Afsharimani B, Cabot P and Parat MO. Morphine and tumor growth and metastasis. Cancer Metastasis Rev 2011; 30: 225-238.

[12] Lennon FE, Mirzapoiazova T, Mambetsariev B, Salgia R, Moss J and Singleton PA. Overexpression of the μ-opioid receptor in human non-small cell lung cancer promotes Akt and mTOR activation, tumor growth, and metastasis. Anesthesiology 2012; 116: 857-867.

[13] Stamer UM, Book M, Comos C, Zhang L, Nauck F and Stüber F. Expression of the nociceptin precursor and nociceptin receptor is modulated in cancer and septic patients. Br J Anaesth 2011; 106: 566-572.

[14] Ishikawa R, Imai A, Mima M, Yamada S, Takeuchi K, Mochizuki D, Shinmura D, Kita JY, Nakagawa T, Kurokawa T, Misawa Y, Nakanishi H, Takizawa Y and Misawa K. Novel prognostic value and potential utility of opioid receptor gene methylation in liquid biopsy for oral cavity cancer. Curr Probl Cancer 2022; 46: 100834.

[15] Chaturvedi M, Schilling J, Beautrait A, Bouvier M, Benovic JL and Shukla AK. Emerging paradigm of intracellular targeting of G protein-coupled receptors. Trends Biochem Sci 2018; 43: 533-546.

[16] Li JX, Bi YP, Wang J, Yang X, Tian YF and Sun ZF. JTC-801 inhibits the proliferation and metastasis of ovarian cancer cell SKOV3 through inhibition of the PI3K - AKT signaling pathway. Pharmazie 2018; 73: 283-287.

[17] Song X, Zhu S, Xie Y, Liu J, Sun L, Zeng D, Wang P, Ma X, Kroemer G, Bartlett DL, Billiar TR, Lotze MT, Zeh HJ, Kang R and Tang D. JTC801

induces pH-dependent death specifically in cancer cells and slows growth of tumors in mice. Gastroenterology 2018; 154: 1480-1493.
[18] Wang S, Ma L, Wang Z, He H, Chen H, Duan Z, Li Y, Si Q, Chuang TH, Chen C and Luo Y. Lactate dehydrogenase-A (LDH-A) preserves cancer stemness and recruitment of tumor-associated macrophages to promote breast cancer progression. Front Oncol 2021; 11: 654452.
[19] Huang X, Xie X, Wang H, Xiao X, Yang L, Tian Z, Guo X, Zhang L, Tang H and Xie X. PDL1 And LDHA act as ceRNAs in triple negative breast cancer by regulating miR-34a. J Exp Clin Cancer Res 2017; 36: 129.
[20] Shen HC, Chen ZQ, Liu XC, Guan JF, Xie DZ, Li YY and Xu C. Sodium oxamate reduces lactate production to improve the glucose homeostasis of Micropterus salmoides fed high-carbohydrate diets. Am J Physiol Regul Integr Comp Physiol 2023; 324: R227-R241.
[21] Feng Y, Ke C, Tang Q, Dong H, Zheng X, Lin W, Ke J, Huang J, Yeung SC and Zhang H. Metformin promotes autophagy and apoptosis in esophageal squamous cell carcinoma by downregulating Stat3 signaling. Cell Death Dis 2014; 5: e1088.
[22] Zhao Z, Han F, Yang S, Wu J and Zhan W. Oxamate-mediated inhibition of lactate dehydrogenase induces protective autophagy in gastric cancer cells: involvement of the Akt-mTOR signaling pathway. Cancer Lett 2015; 358: 17-26.
[23] Chiche J, Ilc K, Laferrière J, Trottier E, Dayan F, Mazure NM, Brahimi-Horn MC and Pouysségur J. Hypoxia-inducible carbonic anhydrase IX and XII promote tumor cell growth by counteracting acidosis through the regulation of the intracellular pH. Cancer Res 2009; 69: 358-368.
[24] Parks SK, Chiche J and Pouyssegur J. pH control mechanisms of tumor survival and growth. J Cell Physiol 2011; 226: 299-308.
[25] Li CY, Anuraga G, Chang CP, Weng TY, Hsu HP, Ta HDK, Su PF, Chiu PH, Yang SJ, Chen FW, Ye PH, Wang CY and Lai MD. Repurposing nitric oxide donating drugs in cancer therapy through immune modulation. J Exp Clin Cancer Res 2023; 42: 22.
[26] Wang CY, Chiao CC, Phan NN, Li CY, Sun ZD, Jiang JZ, Hung JH, Chen YL, Yen MC, Weng TY, Chen WC, Hsu HP and Lai MD. Gene signatures and potential therapeutic targets of amino acid metabolism in estrogen receptor-positive breast cancer. Am J Cancer Res 2020; 10: 95-113.
[27] Xuan DTM, Wu CC, Wang WJ, Hsu HP, Ta HDK, Anuraga G, Chiao CC and Wang CY. Glutamine synthetase regulates the immune microenvironment and cancer development through the inflammatory pathway. Int J Med Sci 2023; 20: 35-49.
[28] Wang CY, Li CY, Hsu HP, Cho CY, Yen MC, Weng TY, Chen WC, Hung YH, Lee KT, Hung JH, Chen YL and Lai MD. PSMB5 plays a dual role in cancer development and immunosuppression. Am J Cancer Res 2017; 7: 2103-2120.
[29] Xuan DTM, Yeh IJ, Su CY, Liu HL, Ta HDK, Anuraga G, Chiao CC, Wang CY and Yen MC. Prognostic and immune infiltration value of proteasome assembly chaperone (PSMG) family genes in lung adenocarcinoma. Int J Med Sci 2023; 20: 87-101.
[30] Lin YY, Wang CY, Phan NN, Chiao CC, Li CY, Sun Z, Hung JH, Chen YL, Yen MC, Weng TY, Hsu HP and Lai MD. PODXL2 maintains cellular stemness and promotes breast cancer development through the Rac1/Akt pathway. Int J Med Sci 2020; 17: 1639-1651.
[31] Barretina J, Caponigro G, Stransky N, Venkatesan K, Margolin AA, Kim S, Wilson CJ, Lehár J, Kryukov GV, Sonkin D, Reddy A, Liu M, Murray L, Berger MF, Monahan JE, Morais P, Meltzer J, Korejwa A, Jané-Valbuena J, Mapa FA, Thibault J, Bric-Furlong E, Raman P, Shipway A, Engels IH, Cheng J, Yu GK, Yu J, Aspesi P Jr, de Silva M, Jagtap K, Jones MD, Wang L, Hatton C, Palescandolo E, Gupta S, Mahan S, Sougnez C, Onofrio RC, Liefeld T, MacConaill L, Winckler W, Reich M, Li N, Mesirov JP, Gabriel SB, Getz G, Ardlie K, Chan V, Myer VE, Weber BL, Porter J, Warmuth M, Finan P, Harris JL, Meyerson M, Golub TR, Morrissey MP, Sellers WR, Schlegel R and Garraway LA. The cancer cell line encyclopedia enables predictive modelling of anticancer drug sensitivity. Nature 2012; 483: 603-607.
[32] Győrffy B. Survival analysis across the entire transcriptome identifies biomarkers with the highest prognostic power in breast cancer. Comput Struct Biotechnol J 2021; 19: 4101-4109.
[33] Durinck S, Spellman PT, Birney E and Huber W. Mapping identifiers for the integration of genomic datasets with the R/bioconductor package biomaRt. Nat Protoc 2009; 4: 1184-1191.
[34] Gentleman RC, Carey VJ, Bates DM, Bolstad B, Dettling M, Dudoit S, Ellis B, Gautier L, Ge Y, Gentry J, Hornik K, Hothorn T, Huber W, Iacus S, Irizarry R, Leisch F, Li C, Maechler M, Rossini AJ, Sawitzki G, Smith C, Smyth G, Tierney L, Yang JY and Zhang J. Bioconductor: open software development for computational biology and bioinformatics. Genome Biol 2004; 5: R80.
[35] Liu HL, Yeh IJ, Phan NN, Wu YH, Yen MC, Hung JH, Chiao CC, Chen CF, Sun Z, Jiang JZ, Hsu HP, Wang CY and Lai MD. Gene signatures of SARS-CoV/SARS-CoV-2-infected ferret lungs in

short- and long-term models. Infect Genet Evol 2020; 85: 104438.
[36] Huang da W, Sherman BT and Lempicki RA. Systematic and integrative analysis of large gene lists using DAVID bioinformatics resources. Nat Protoc 2009; 4: 44-57.
[37] Huang da W, Sherman BT and Lempicki RA. Bioinformatics enrichment tools: paths toward the comprehensive functional analysis of large gene lists. Nucleic Acids Res 2009; 37: 1-13.
[38] Kao TJ, Wu CC, Phan NN, Liu YH, Ta HDK, Anuraga G, Wu YF, Lee KH, Chuang JY and Wang CY. Prognoses and genomic analyses of proteasome 26S subunit, ATPase (PSMC) family genes in clinical breast cancer. Aging (Albany NY) 2021; 13: 17970.
[39] Xuan DTM, Yeh IJ, Wu CC, Su CY, Liu HL, Chiao CC, Ku SC, Jiang JZ, Sun Z, Ta HDK, Anuraga G, Wang CY and Yen MC. Comparison of transcriptomic signatures between monkeypox-infected monkey and human cell lines. J Immunol Res 2022; 2022: 3883822.
[40] Wu YH, Yeh IJ, Phan NN, Yen MC, Hung JH, Chiao CC, Chen CF, Sun Z, Hsu HP, Wang CY and Lai MD. Gene signatures and potential therapeutic targets of Middle East respiratory syndrome coronavirus (MERS-CoV)-infected human lung adenocarcinoma epithelial cells. J Microbiol Immunol Infect 2021; 54: 845-857.
[41] Ashburner M, Ball CA, Blake JA, Botstein D, Butler H, Cherry JM, Davis AP, Dolinski K, Dwight SS, Eppig JT, Harris MA, Hill DP, Issel-Tarver L, Kasarskis A, Lewis S, Matese JC, Richardson JE, Ringwald M, Rubin GM and Sherlock G. Gene ontology: tool for the unification of biology. The Gene Ontology Consortium. Nat Genet 2000; 25: 25-29.
[42] Subramanian A, Tamayo P, Mootha VK, Mukherjee S, Ebert BL, Gillette MA, Paulovich A, Pomeroy SL, Golub TR, Lander ES and Mesirov JP. Gene set enrichment analysis: a knowledge-based approach for interpreting genome-wide expression profiles. Proc Natl Acad Sci U S A 2005; 102: 15545-15550.
[43] Tsai YT, Li CY, Huang YH, Chang TS, Lin CY, Chuang CH, Wang CY, Anuraga G, Chang TH, Shih TC, Lin ZY, Chen YL, Chung I, Lee KH, Chang CC, Sung SY, Yang KH, Tsui WL, Yap CV and Wu MH. Galectin-1 orchestrates an inflammatory tumor-stroma crosstalk in hepatoma by enhancing TNFR1 protein stability and signaling in carcinoma-associated fibroblasts. Oncogene 2022; 41: 3011-3023.
[44] Anuraga G, Wang WJ, Phan NN, An Ton NT, Ta HDK, Berenice Prayugo F, Minh Xuan DT, Ku SC, Wu YF, Andriani V, Athoillah M, Lee KH and Wang CY. Potential prognostic biomarkers of NIMA (Never in Mitosis, Gene A)-related kinase (NEK) family members in breast cancer. J Pers Med 2021; 11: 1089.
[45] Hagerling C, Gonzalez H, Salari K, Wang CY, Lin C, Robles I, van Gogh M, Dejmek A, Jirström K and Werb Z. Immune effector monocyte-neutrophil cooperation induced by the primary tumor prevents metastatic progression of breast cancer. Proc Natl Acad Sci U S A 2019; 116: 21704-21714.
[46] Owyong M, Chou J, van den Bijgaart RJ, Kong N, Efe G, Maynard C, Talmi-Frank D, Solomonov I, Koopman C, Hadler-Olsen E, Headley M, Lin C, Wang CY, Sagi I, Werb Z and Plaks V. MMP9 modulates the metastatic cascade and immune landscape for breast cancer anti-metastatic therapy. Life Sci Alliance 2019; 2: e201800226.
[47] Wang CY, Chang YC, Kuo YL, Lee KT, Chen PS, Cheung CHA, Chang CP, Phan NN, Shen MR and Hsu HP. Mutation of the PTCH1 gene predicts recurrence of breast cancer. Sci Rep 2019; 9: 16359.
[48] Hill DP, D'Eustachio P, Berardini TZ, Mungall CJ, Renedo N and Blake JA. Modeling biochemical pathways in the gene ontology. Database (Oxford) 2016; 2016: baw126.
[49] Huang X, Li X, Xie X, Ye F, Chen B, Song C, Tang H and Xie X. High expressions of LDHA and AMPK as prognostic biomarkers for breast cancer. Breast 2016; 30: 39-46.
[50] Sun X, Wang M, Wang M, Yu X, Guo J, Sun T, Li X, Yao L, Dong H and Xu Y. Metabolic reprogramming in triple-negative breast cancer. Front Oncol 2020; 10: 428.
[51] Chen F, Chen J, Yang L, Liu J, Zhang X, Zhang Y, Tu Q, Yin D, Lin D, Wong PP, Huang D, Xing Y, Zhao J, Li M, Liu Q, Su F, Su S and Song E. Extracellular vesicle-packaged HIF-1α-stabilizing lncRNA from tumour-associated macrophages regulates aerobic glycolysis of breast cancer cells. Nat Cell Biol 2019; 21: 498-510.
[52] Li W, Tanikawa T, Kryczek I, Xia H, Li G, Wu K, Wei S, Zhao L, Vatan L, Wen B, Shu P, Sun D, Kleer C, Wicha M, Sabel M, Tao K, Wang G and Zou W. Aerobic glycolysis controls myeloid-derived suppressor cells and tumor immunity via a specific CEBPB isoform in triple-negative breast cancer. Cell Metab 2018; 28: 87-103, e106.
[53] García-Castillo V, López-Urrutia E, Villanueva-Sánchez O, Ávila-Rodríguez MÁ, Zentella-Dehesa A, Cortés-González C, López-Camarillo C, Jacobo-Herrera NJ and Pérez-Plasencia C. Targeting metabolic remodeling in triple negative breast cancer in a murine model. J Cancer 2017; 8: 178-189.
[54] Zakaria S, Elsebaey S, Allam S, Abdo W and El-Sisi A. Siah2 inhibitor and the metabolic antagonist Oxamate retard colon cancer progression and downregulate PD1 expression. Recent Pat Anticancer Drug Discov 2023; [Epub ahead of print].

[55] Oginuma M, Harima Y, Tarazona OA, Diaz-Cuadros M, Michaut A, Ishitani T, Xiong F and Pourquié O. Intracellular pH controls WNT downstream of glycolysis in amniote embryos. Nature 2020; 584: 98-101.
[56] Parks SK, Chiche J and Pouysségur J. Disrupting proton dynamics and energy metabolism for cancer therapy. Nat Rev Cancer 2013; 13: 611-623.
[57] Chiche J, Le Fur Y, Vilmen C, Frassineti F, Daniel L, Halestrap AP, Cozzone PJ, Pouysségur J and Lutz NW. In vivo pH in metabolic-defective ras-transformed fibroblast tumors: key role of the monocarboxylate transporter, MCT4, for inducing an alkaline intracellular pH. Int J Cancer 2012; 130: 1511-1520.

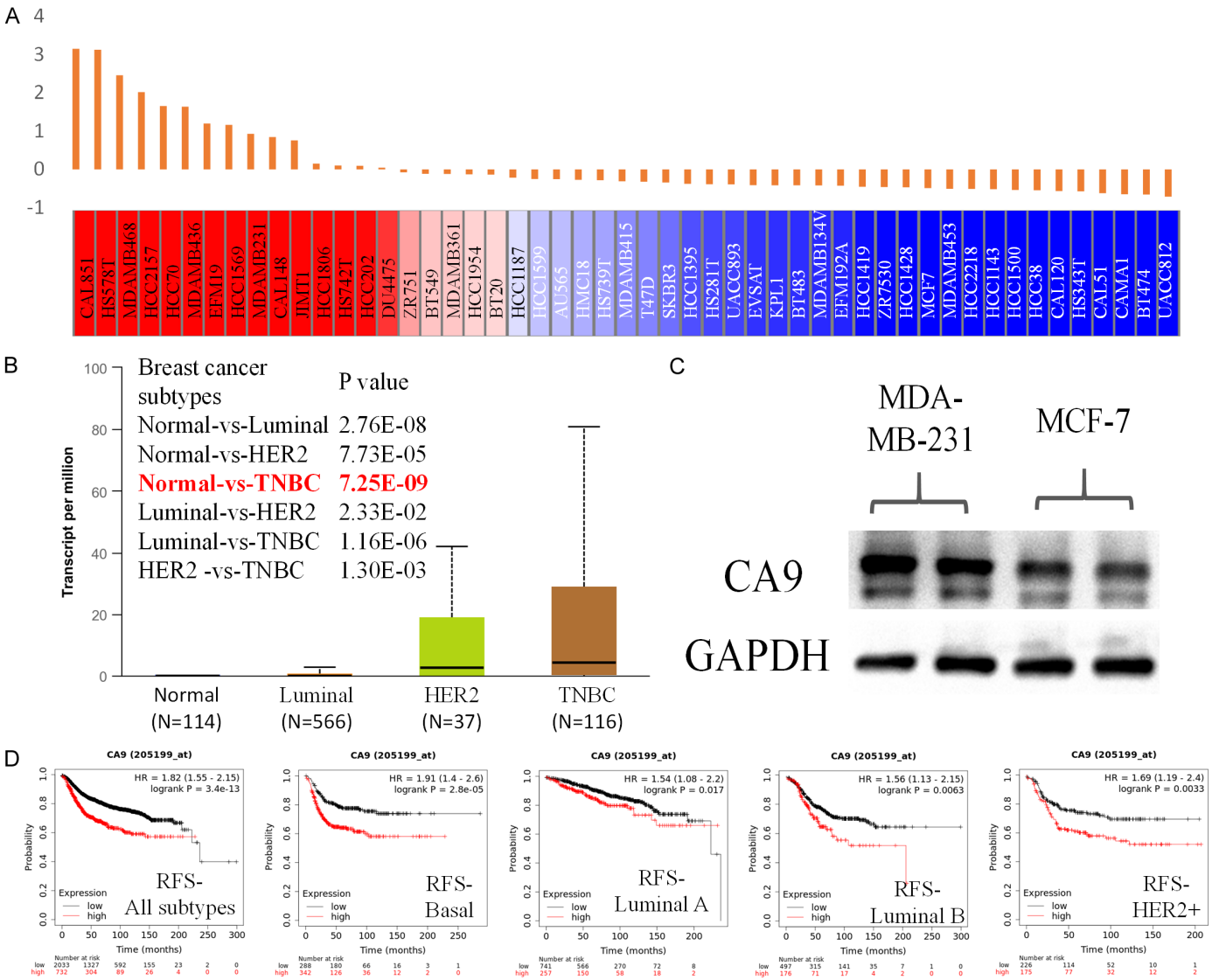

Supplementary Figure 1. The JTC-801-induced cell death marker, CA9, had high expression in triple-negative breast cancer (TNBC) and further caused poor prognoses. A. RNA-Sequencing analysis of CA9 mRNA in different breast cancer cell lines in the Cancer Cell Line Encyclopedia (CCLE). Red indicates overexpression (left), while blue indicates downregulation (right) of CA9 in each cancer cell line. B. Expression of CA9 in distinct subtypes of breast cancer. A one-way ANOVA was conducted to calculate *p* values between groups. C. CA9 protein levels of different breast cancer cell lines were evaluated by Western blotting. Three independent experiments were performed, and GAPDH was used as an internal control. These data indicated that the TNBC cell line (MDA-MB-231) had higher expression of CA9 (JTC-801 induced marker) compared to the luminal cell line (MCF-7). D. Disease-free survival curve from the Kaplan-Meier Plotter and evaluation of impacts from low (black line) and high (red line) expressions of CA9 in different subtypes of breast cancer.

A

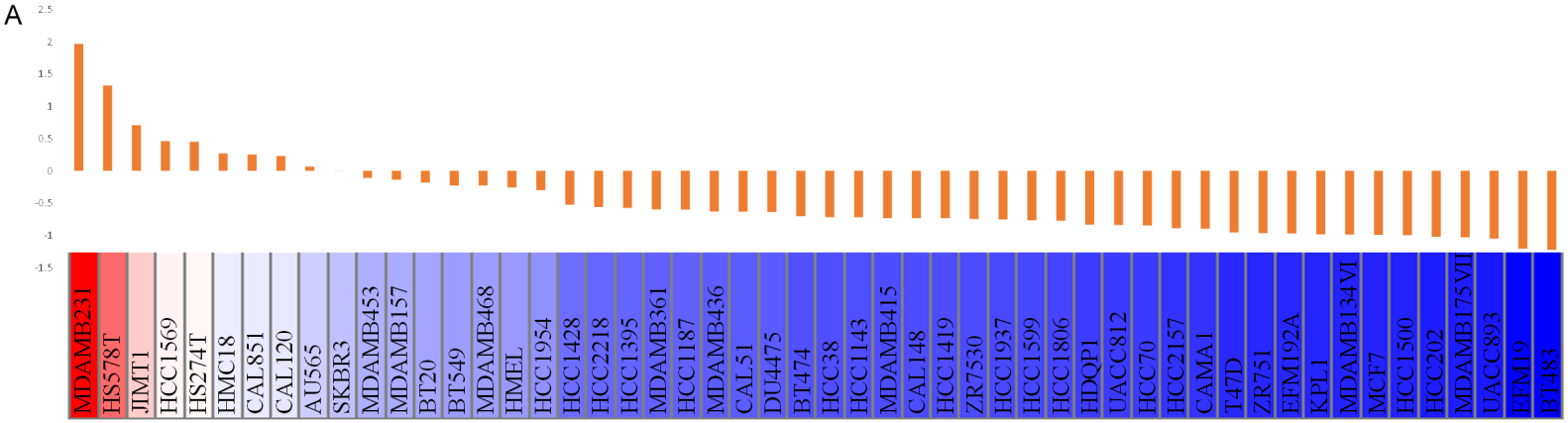
MDAMB231
HS578T
JIMT1
HCC1569
HS274T
HMC18
CAL851
CAL120
AU565
SKBR3
MDAMB453
MDAMB157
BT20
BT549
MDAMB468
HMEL
HCC1954
HCC1428
HCC2218
HCC1395
MDAMB361
HCC1187
MDAMB436
CAL51
DU4475
BT474
HCC38
HCC1143
MDAMB415
CAL148
HCC1419
ZR7530
HCC1937
HCC1599
HCC1806
HDQP1
UACC812
HCC70
HCC2157
CAMA1
T47D
ZR751
EFM192A
KPL1
MDAMB134VI
MCF7
HCC1500
HCC202
MDAMB175VII
UACC893
EFM19
BT483

B

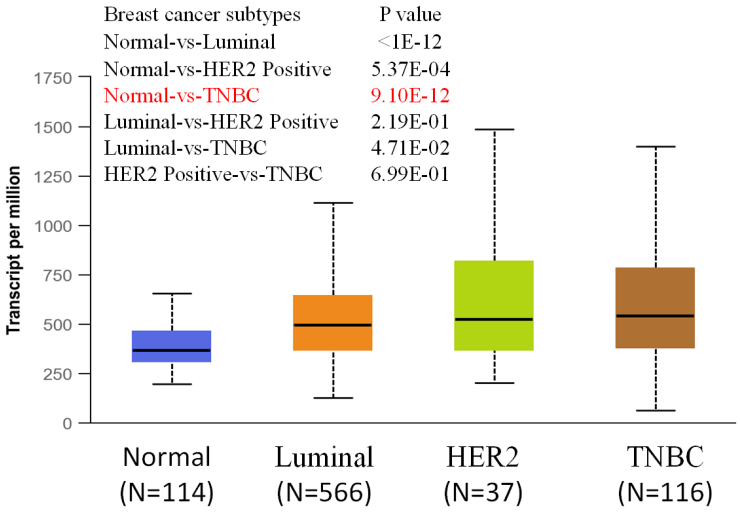
Breast cancer subtypes
P value
Normal-vs-Luminal
<1E-12
Normal-vs-HER2 Positive
5.37E-04
Normal-vs-TNBC
9.10E-12
Luminal-vs-HER2 Positive
2.19E-01
Luminal-vs-TNBC
4.71E-02
HER2 Positive-vs-TNBC
6.99E-01
Transcript per million
Normal (N=114)
Luminal (N=566)
HER2 (N=37)
TNBC (N=116)

C

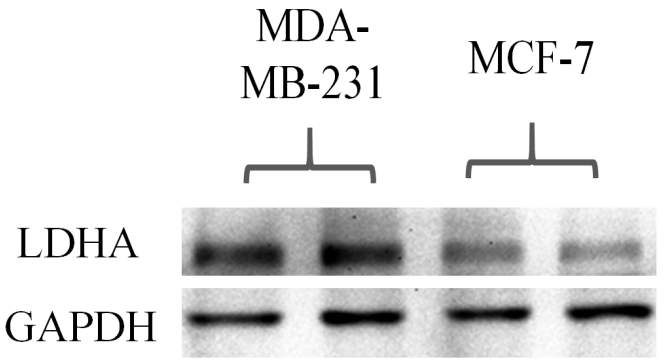
MDA-MB-231
MCF-7
LDHA
GAPDH

D

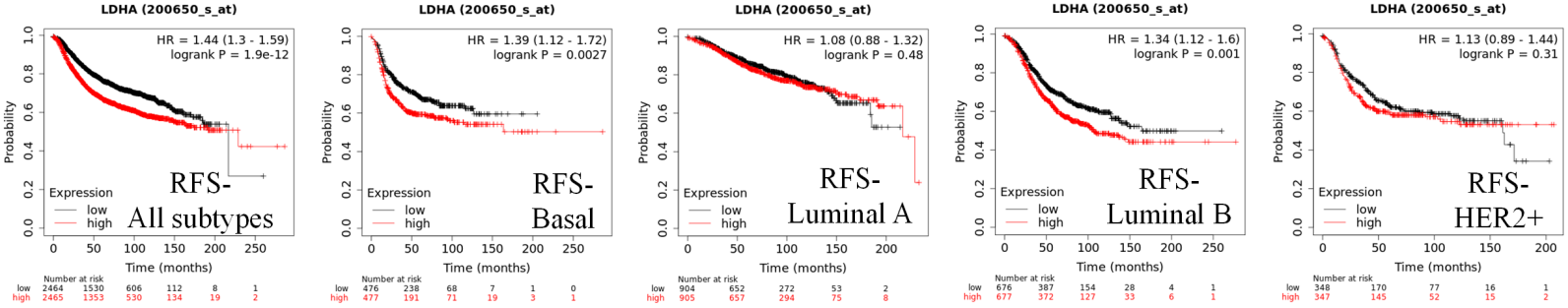
LDHA (200650_s_at)
HR = 1.44 (1.3 - 1.59)
logrank P = 1.9e-12
RFS-All subtypes
HR = 1.39 (1.12 - 1.72)
logrank P = 0.0027
RFS-Basal
HR = 1.08 (0.88 - 1.32)
logrank P = 0.48
RFS-Luminal A
HR = 1.34 (1.12 - 1.6)
logrank P = 0.001
RFS-Luminal B
HR = 1.13 (0.89 - 1.44)
logrank P = 0.31
RFS-HER2+
Probability
Expression
low
high
Time (months)
Number at risk

Supplementary Figure 2. The sodium oxamate-induced cell death marker, lactate dehydrogenase A (LDHA), had high expression in triple-negative breast cancer (TNBC) and further caused poor prognoses. A. RNA-Sequencing analysis of LDHA mRNA in different breast cancer cell lines in the Cancer Cell Line Encyclopedia (CCLE). Red indicates overexpression (left), while blue indicates downregulation (right) of LDHA in each cancer cell line. B. Expressions of LDHA in distinct subtypes of breast cancer. A one-way ANOVA was conducted to calculate *p* values between groups. C. LDHA protein levels of different breast cancer cell lines were evaluated by Western blotting. Three independent experiments were performed, and GAPDH was used as an internal control. These data indicated that the TNBC cell line (MDA-MB-231) had higher expression of LDHA (a sodium oxamate-induced marker) compared to the luminal cell line (MCF-7). D. Disease-free survival curve from the Kaplan-Meier Plotter and evaluation of the impact from low (black line) and high (red line) expression levels of LDHA in different subtypes of breast cancer.

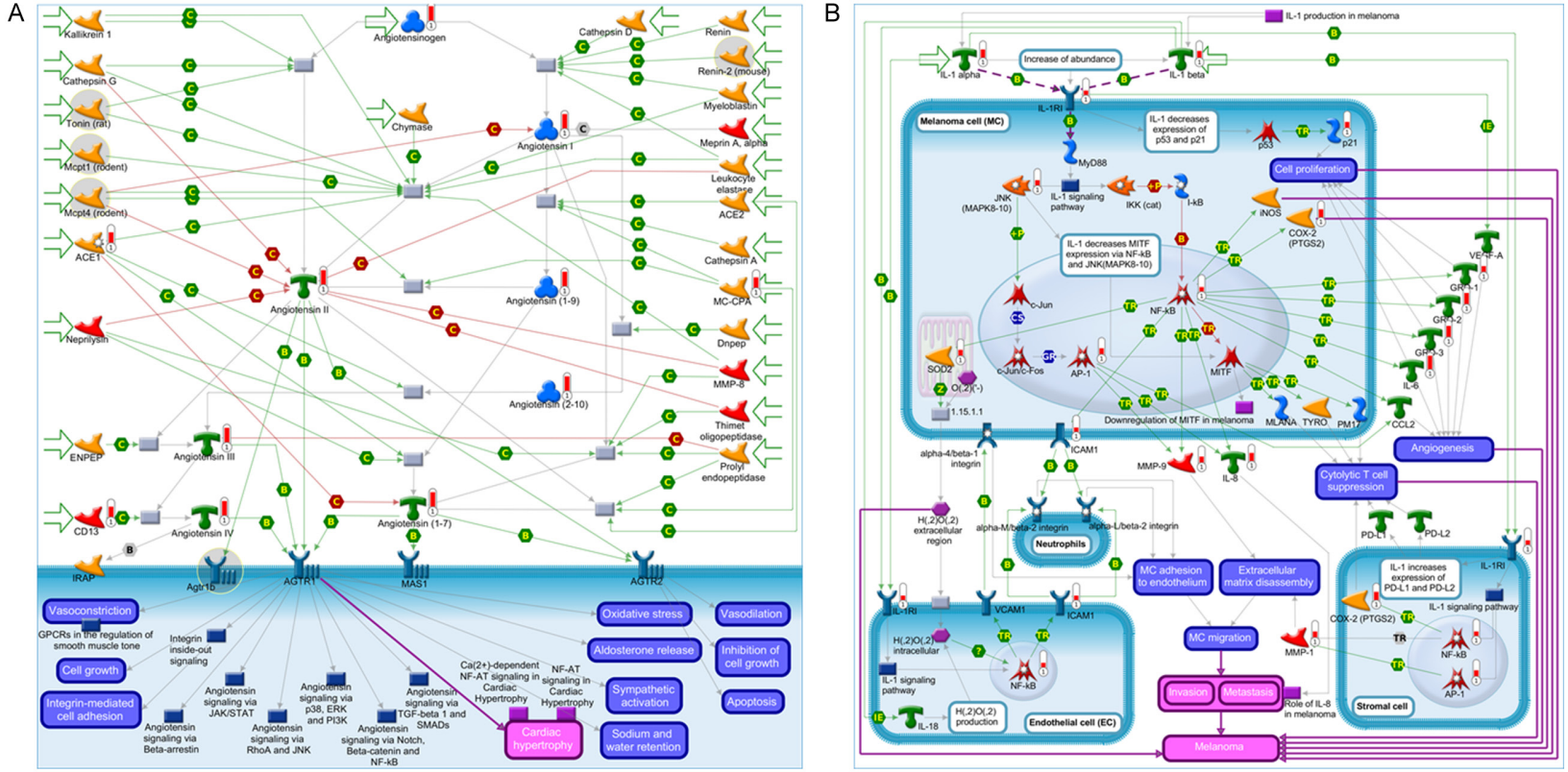

Supplementary Figure 3. MetaCore pathway analysis of JTC-801-treated MDA-MB-231 cells. A. “Protein folding and maturation_Angiotensin system maturation” was listed as the most downregulated pathway after JTC-801 treatment. B. “IL-1 signaling” was listed as the most downregulated pathway after JTC-801 treatment.

Supplementary Table 1. Top 25 downregulated pathways in the MetaCore analysis of potential maps when comparing JTC-801-treated MDA-MB-231 cells with the control group

Rank	Maps	*P* value	Network objects from active data
1	Protein folding and maturation_Angiotensin system maturation	7.13E-08	Angiotensin III, Angiotensin (2-10), Angiotensinogen, ACE1, MC-CPA, Angiotensin IV, Angiotensin I, Angiotensin II, Angiotensin (1-7), Angiotensin (1-9), CD13
2	Eosinophil granule protein release in asthma	1.83E-05	FPRL1, ST2(L), CRLF2, cPKC (conventional), PKC, CCR3, CRTH2, FPR, NT-3
3	Cell adhesion_Classical cadherin-mediated cell adhesion	7.05E-05	VE-cadherin, N-cadherin, Actin cytoskeletal, Alpha-actinin, F-Actin, F-Actin cytoskeleton
4	Eosinophil survival in asthma	1.06E-04	PGE2R2, ST2(L), CRLF2, iNOS, Eotaxin-2, TrkB, CCR3, PGD2R, NT-3
5	GTP metabolism	1.28E-04	PDE6B, PDE6A, PDE6G, Guanylate cyclase C (GC-C), ENP1, PDE10A, NDPK B, PDE6H
6	G-protein signaling_RhoA activation	1.53E-04	RhoN, VE-cadherin, N-cadherin, NGFR(TNFRSF16), Cyclin B, Thrombin, Ephrin-A, Angiotensin II, IGF-1, VAV-1
7	Signal transduction_WNT/Beta-catenin signaling in tissue homeostasis	1.58E-04	FGF18, iNOS, Claudin-2, Tcf(Lef), ROR-gamma, TCF7L2 (TCF4), Versican
8	Development_Direct reprogramming of cardiac fibroblasts into cardiomyocytes	1.93E-04	Alpha-actinin 2, MLC2, c-Kit, Thy-1, Troponin I, slow skeletal
9	Cell adhesion_Tight junctions	2.14E-04	Actin cytoskeletal, Tubulin alpha, F-Actin, Claudin-2, PARD6, Actin, MRLC
10	Protein folding and maturation_Bradykinin/Kallidin maturation	2.40E-04	BDKRB1, ACE1, BDKRB2, Plasmin, Plasma kallikrein, CD13
11	Development_Androgen receptor in reproductive system development	4.18E-04	Androgen receptor, N-cadherin, Eppin, Amphiregulin, RelA (p65 NF-kB subunit), MafB, IGF-1, Claudin-3, CYP19
12	CHDI_Correlations from Replication data_Cytoskeleton and adhesion module	4.25E-04	Plasminogen, Actin cytoskeletal, MHC class II, Alpha-actinin, Plasmin, Ephrin-B, VAV-1, MRLC
13	Macrophage and dendritic cell phenotype shift in cancer	5.27E-04	PGE2R2, EPAS1, IDO1, MHC class II, RelA (p65 NF-kB subunit), TLR7, NF-kB, iNOS, SHIP, IL-10
14	Fibroblast/myofibroblast proliferation in asthmatic airways	5.47E-04	BDKRB1, NF-kB, PKC, FGFR2, Thrombin, IGF-1
15	Role of neuropeptides in pathogenesis of SCLC	5.81E-04	BDKRB1, GRP-R, cPKC (conventional), BDKRB2, NMB-R, PKC, GALR2, NTSR1
16	B-regulatory cells and tumor cells intercellular interaction	5.81E-04	OX40L(TNFSF4), FPRL1, ST2(L), RelA (p65 NF-kB subunit), TLR7, NF-kB, IL-10, NF-kB p65/p65
17	Cell adhesion_Endothelial cell contacts by junctional mechanisms	7.13E-04	VE-cadherin, N-cadherin, Actin cytoskeletal, Alpha-actinin, Claudin-3
18	Signal transduction_FGFR2 signaling	7.20E-04	cPKC (conventional), FGF18, RelA (p65 NF-kB subunit), FGF7, PKC, FGFR2, Klotho beta, FGF12, Osteocalcin, Aquaporin 3
19	Regulatory T cells in human allergic contact dermatitis	7.24E-04	MHC class II, CCR7, IL-10
20	Immune response_CCL2 signaling	7.76E-04	VE-cadherin, Actin cytoskeletal, Cadherin 12, NF-kB, iNOS, CCBP2 (CCR9), CDH19
21	Th2-cytokine-induced airway epithelium mucous metaplasia in COPD	7.82E-04	Actin cytoskeletal, TMEM16A, NF-kB, iNOS, HAG-2, nNOS, Mucin 5AC, NF-kB p65/p65
22	Inhibition of neutrophil migration by proresolving lipid mediators in COPD	8.60E-04	FPRL1, Actin cytoskeletal, cPKC (conventional), Alpha-actinin, NF-kB, PKC, VAV-1, FPR
23	Regulation of metabolism_GLP-1 signaling in beta cells	1.08E-03	EGR1, GLP-1 (7-37), PTPRN, Amylin, NF-kB, PGAM2, TCF7L2 (TCF4), Menin, GLP-1 (7-36) amide
24	Gamma-Secretase regulation of neuronal cell development and function	1.08E-03	Transgelin, N-cadherin, NGFR (ICD), N-cadherin (CTF1), N-cadherin (CTF2), NGFR(TNFRSF16), NGFR (CTF)
25	Apoptosis and survival_Anti-apoptotic TNFs/NF-kB/Bcl-2 pathway	1.10E-03	OX40L(TNFSF4), BCMA(TNFRSF17), NGFR(TNFRSF16), RelA (p65 NF-kB subunit), NF-kB, TRAF3

Statistical significance was set to $P < 0.05$.

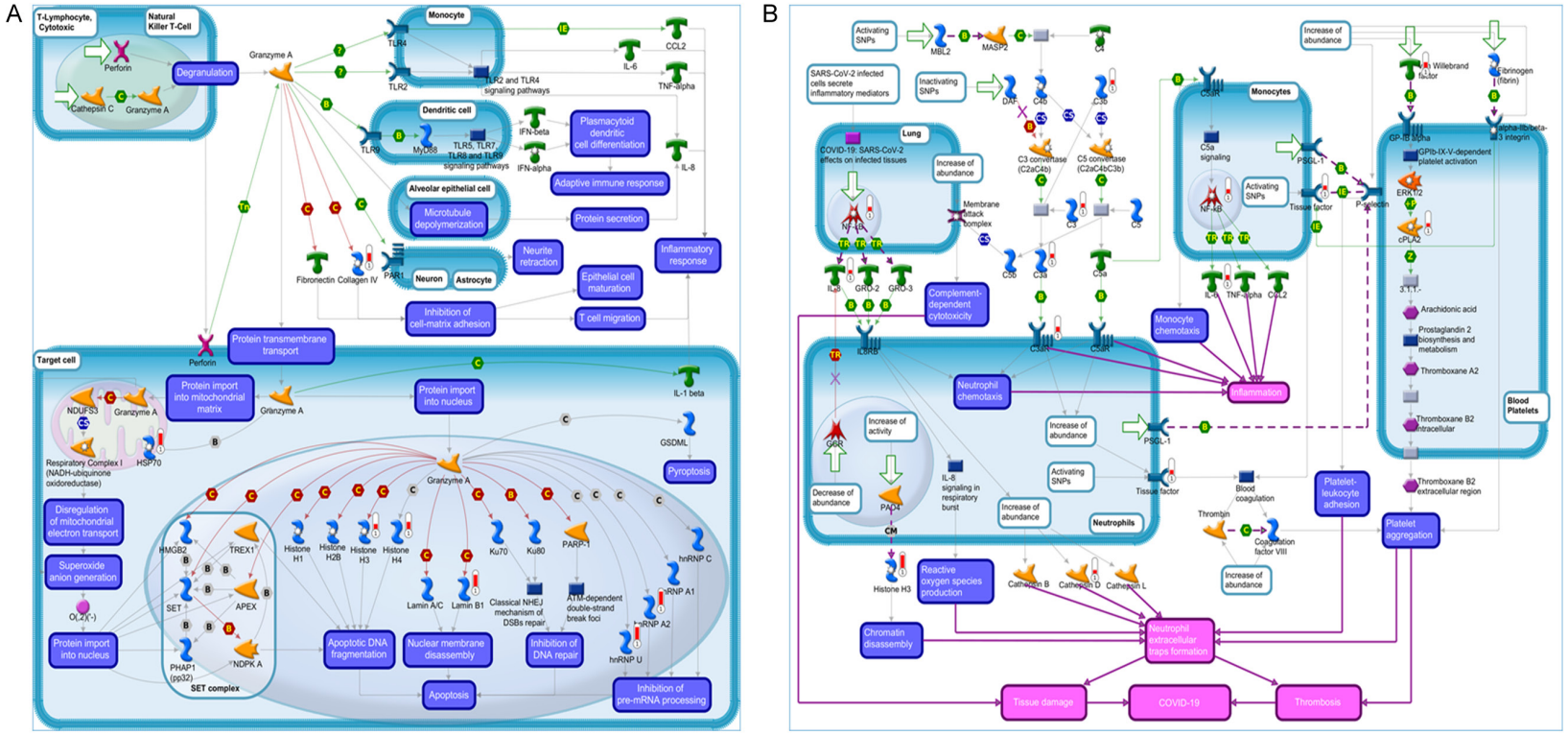

Supplementary Figure 4. MetaCore pathway analysis of sodium oxamate-treated MDA-MB-231 cells. A. “Apoptosis and survival_Granzyme A signaling” was listed as the most downregulated pathway after sodium oxamate treatment. B. “COVID-19 associated coagulopathy” was listed as the top upregulated pathway after sodium oxamate treatment.

Supplementary Table 2. Top 25 downregulated pathways in the MetaCore analysis of potential maps when comparing sodium oxamate-treated MDA-MB-231 cells with control group

Rank	Maps	*P* value	Network objects from active data
1	Apoptosis and survival_Granzyme A signaling	3.50E-05	hnRNP U, Histone H3, Collagen IV, HSP70, hnRNP A2, Histone H4, Lamin B1
2	Muscle contraction_GPCRs in the regulation of smooth muscle tone	1.13E-04	PGE2R2, Myosin II, MaxiK alpha subunit, PLC-beta, MELC, MyHC, NCX1, MLCK, MRLC
3	Airway smooth muscle contraction in asthma	2.70E-04	PGE2R2, Myosin II, PLC-beta, MELC, MyHC, MLCK, MRLC
4	Development_Androgen receptor in reproductive system development	4.72E-04	N-cadherin, Claudin-11, Eppin, MafB, OSCP1, IGF-1, LRH1, Connexin 43
5	Cell adhesion_Histamine H1 receptor signaling in the interruption of cell barrier integrity	5.21E-04	VE-cadherin, Myosin II, PLC-beta, MELC, MLCK, MRLC
6	Populations of skin dendritic cells involved in contact hypersensitivity	6.35E-04	Ep-CAM, MHC class II, CCR6, CD36
7	Cytoskeleton remodeling_Alpha-1A adrenergic receptor-dependent inhibition of PI3K	7.90E-04	Myosin II, MELC, MLCK, MRLC
8	Calcium-dependent regulation of normal and asthmatic smooth muscle contraction	8.93E-04	Myosin II, Thrombin, PLC-beta, CD38, NCX1, MLCK, MRLC
9	Role of tumor-infiltrating B cells in anti-tumor immunity	1.11E-03	IL-18R1, MHC class II, AID, CT47A, CD20, CD38, Btk, MAGEA10
10	Neurophysiological process_Long-term depression in cerebellum	1.26E-03	Corticoliberin, GRID2, PLC-beta, PIB4, IGF-1, P/Q-type calcium channel alpha-1A subunit
11	Immune response_Antigen presentation by MHC class II	1.53E-03	MHC class II alpha chain, HLA-DO, MHC class II, HSP90, MHC class II beta chain, Kinesin heavy chain, Endoplasmin, CD79B, MAP1LC3A
12	Development_NOTCH signaling in organogenesis and embryogenesis	1.86E-03	VE-cadherin, Islet-1, HEY2, TIE2, Neuregulin 1, VEGFR-3, Connexin 43
13	Immune response _CCR3 signaling in eosinophils	1.86E-03	Myosin II, Eotaxin-2, CCR3, MELC, MyHC, MLCK, MRLC
14	B cell signaling in hematological malignancies	1.86E-03	APRIL(TNFSF13), CD20, TRAF3, CD38, Btk, CD70(TNFSF7), CD79B
15	Development_SLIT-ROBO1 signaling	2.06E-03	SLIT3, Myosin II, Calcineurin A (catalytic), LSP1, SLIT1
16	Stem cells_Pancreatic cancer stem cells in tumor metastasis	2.06E-03	Myosin II, MELC, MyHC, MLCK, MRLC
17	Development_Regulation of cytoskeleton proteins in oligodendrocyte differentiation and myelination	2.21E-03	Tubulin beta, Myosin II, MAP6, MELC, hnRNP A2, MRLC
18	Hedgehog signaling in prostate cancer	2.69E-03	HIP, GLI-1, HSP90, BMI-1
19	Cell adhesion_Endothelial cell contacts by junctional mechanisms	2.69E-03	VE-cadherin, N-cadherin, JAM2, Connexin 43
20	Regulation of microRNAs in colorectal cancer	2.85E-03	miR-18a-5p, microRNA 19a, miR-19a-3p, microRNA 20a, microRNA 18a, miR-20a-5p
21	Role of TLR signaling in skin sensitization	3.16E-03	TRAM, CD14, TRAF3, HSP70, MEK6(MAP2K6)
22	Role of CD8+ Tc1 cells in COPD	3.16E-03	IL-18R1, CXCL16, Leptin receptor, MIP-1-alpha, KLRK1 (NKG2D)
23	Cell adhesion_Tight junctions	3.16E-03	Myosin II, JAM2, PARD6, DNMBP(TUBA), MRLC
24	Inhibition of remyelination in multiple sclerosis: regulation of cytoskeleton proteins	3.16E-03	Tubulin beta, Myosin II, MELC, hnRNP A2, MRLC
25	Proinflammatory mediators production and activation of basophils in asthma	3.49E-03	ST2(L), MHC class II, Calcineurin A (catalytic), Leptin receptor, ENPP3

Statistical significance was set to $P < 0.05$.

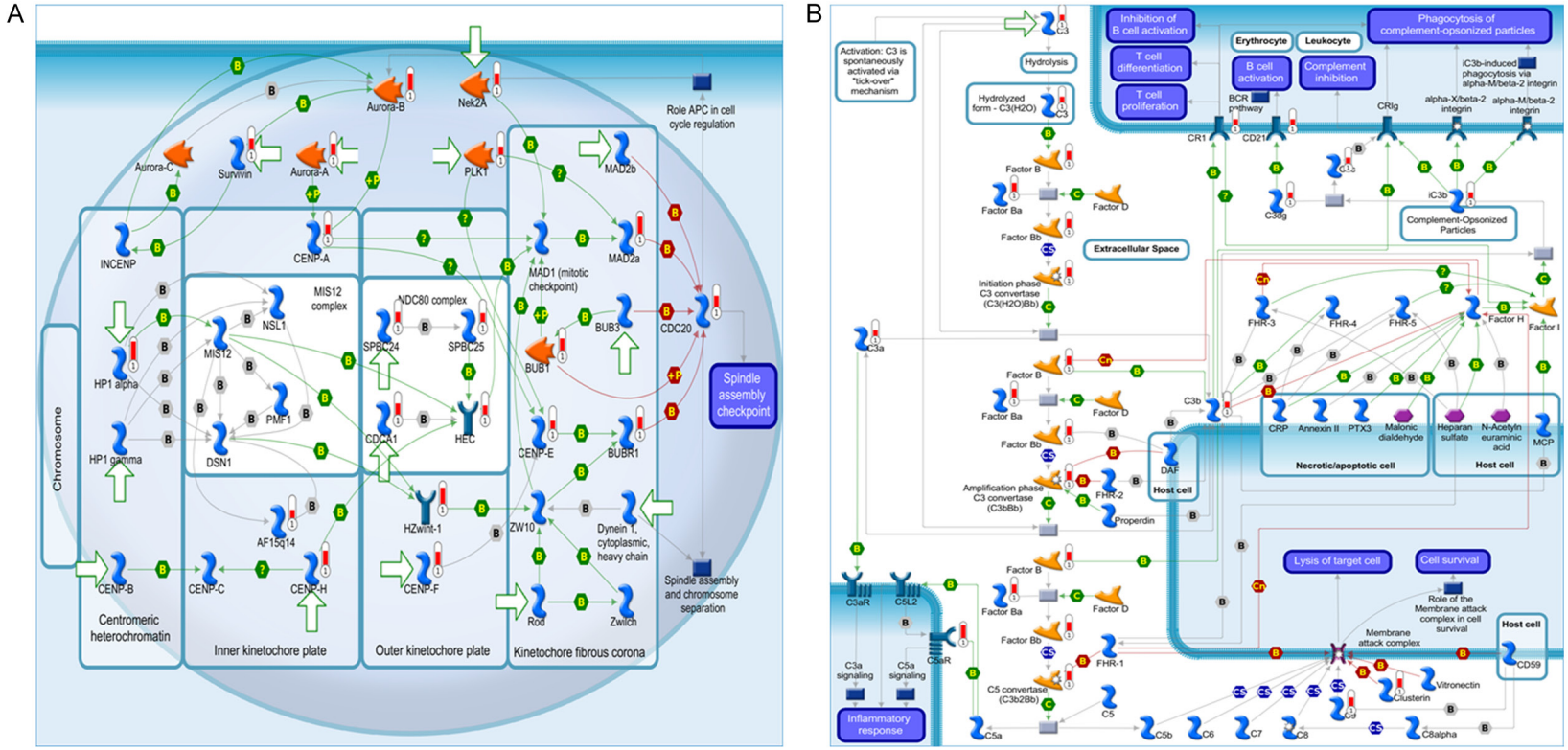

Supplementary Figure 5. MetaCore pathway analysis of JTC-801/sodium oxamate-cotreated MDA-MB-231 cells. A. "Cell cycle_The metaphase checkpoint" was listed as the most downregulated pathway after JTC-801 and sodium oxamate combined treatment. B. "Immune response_Alternative complement pathway" was listed as the top upregulated pathway after JTC-801 and sodium oxamate combined treatment.

Supplementary Table 3. Top 25 downregulated pathways in the MetaCore analysis of potential maps when comparing JTC-801/sodium oxamate-cotreated MDA-MB-231 cells with the control group

Rank	Maps	*P* value	Network objects from active data
1	Cell cycle_The metaphase checkpoint	3.81E-21	SPBC25, Aurora-B, HEC, HZwint-1, Survivin, CENP-E, Nek2A, BUB1, CENP-A, HP1 alpha, SPBC24, Aurora-A, PLK1, CDCA1, CDC20, CENP-F, MAD2a, CENP-H, AF15q14, BUBR1
2	Cell cycle_Chromosome condensation in prometaphase	1.38E-18	CAP-H/H2, Condensin, CAP-C, Cyclin A, CNAP1, CAP-D2/D3, Aurora-B, Cyclin B, TOP2, BRRN1, CAP-G, CAP-G/G2, Aurora-A, CAP-E, CDK1 (p34)
3	Cell cycle_Spindle assembly and chromosome separation	1.85E-14	Importin (karyopherin)-beta, KNSL1, Aurora-B, HEC, Tubulin alpha, Cyclin B, Separase, Nek2A, TPX2, CSE1L, Aurora-A, CDC20, MAD2a, CDK1 (p34), Tubulin (in microtubules)
4	Cell cycle_Role of APC in cell cycle regulation	2.72E-13	Tome-1, Cyclin A, Aurora-B, SKP2, Cyclin B, Nek2A, BUB1, Emi1, Aurora-A, PLK1, CDC20, MAD2a, CDK1 (p34), BUBR1
5	Cell cycle_Role of Nek in cell cycle regulation	3.53E-08	Tubulin beta, HEC, Tubulin alpha, Nek2A, Cyclin B1, TPX2, Aurora-A, MAD2a, CDK1 (p34), Tubulin (in microtubules)
6	DNA damage_ATM/ATR regulation of G2/M checkpoint: nuclear signaling	1.22E-07	Cyclin A, Brca1, Cyclin B, Cyclin B2, TTK, CDC25C, Cyclin B1, PLK1, GTSE1, DNA-PK, CDK1 (p34)
7	DNA damage_ATM/ATR regulation of G2/M checkpoint: cytoplasmic signaling	4.83E-07	BORA, Aurora-B, Brca1/Bard1, Brca1, CDC25C, UBE2C, Cyclin B1, Aurora-A, PLK1, MEK6(MAP2K6), CDK1 (p34)
8	Cell cycle_Initiation of mitosis	9.82E-07	Lamin B, KNSL1, Cyclin B2, CDC25C, Cyclin B1, PLK1, FOXM1, CDK1 (p34)
9	Inhibition of remyelination in multiple sclerosis: regulation of cytoskeleton proteins	8.59E-06	chTOG, Tubulin beta, Tubulin alpha, PKC-alpha, hnRNP A2, Fibronectin, MRLC, Stathmin, Tubulin (in microtubules)
10	Cell cycle_Transition and termination of DNA replication	1.28E-05	TOP2 alpha, Cyclin A, Brca1/Bard1, Brca1, TOP2, Bard1, CDK1 (p34)
11	DNA damage_Double-strand break repair via homologous recombination	1.41E-05	FIGNL1, EXO1, Brca1/Bard1, Brca1, AUNIP, BLM, NUCKS, PIR51, PLK1, MCM8, Histone H4, CDK1 (p34)
12	Reproduction_Progesterone-mediated oocyte maturation	3.26E-05	PKA-reg (cAMP-dependent), CDC25C, BUB1, Cyclin B1, Aurora-A, PLK1, CDC20, CDK1 (p34)
13	DNA damage_G2 checkpoint in response to DNA mismatches	3.56E-05	MutSalpha complex, EXO1, Brca1, MSH2, CDC25C, MSH6, CDK1 (p34)
14	Cell cycle_Cell cycle (generic schema)	3.78E-05	Cyclin A, Cyclin B, E2F2, CDC25C, p107, CDK1 (p34)
15	Cell cycle_Nucleocytoplasmic transport of CDK/Cyclins	5.21E-05	Cyclin A, Karyopherin beta 1, CRM1, Cyclin B1, CDK1 (p34)
16	DNA damage_Intra S-phase checkpoint	1.48E-04	Cyclin A, Brca1, CDC7, MCM5, BLM, FANCD2, MCM4, FANCI (KIAA1794), DNA-PK, CDC45L
17	Transport_The role of AVP in regulation of Aquaporin 2 and renal water reabsorption	1.72E-04	PKA-reg type II (cAMP-dependent), PKA-reg (cAMP-dependent), Calmodulin, PRKAR2B, MyHC, V2 receptor, MLCK, MRLC
18	CHDI_Correlations from Replication data_Causal network (negative correlations)	2.47E-04	Plasminogen, Plasmin, PKC, Fibronectin, TCF7L2 (TCF4), PLC-beta1, ACM3
19	Abnormalities in cell cycle in SCLC	2.66E-04	Cyclin A, Aurora-B, SKP2, E2F2, Cyclin B1, CDK1 (p34)
20	Apoptosis and survival_Granzyme A signaling	2.90E-04	hnRNP U, HMGB2, PARP-1, hnRNP A2, Fibronectin, Histone H4, Lamin B1
21	Oxidative stress_Activation of NOX1, NOX5, DUOX1 and DUOX2 NADPH Oxidases	3.38E-04	cPKC (conventional), PKA-reg (cAMP-dependent), Calmodulin, PKC, PKC-alpha, NOX5, NOXA1
22	Airway smooth muscle contraction in asthma	3.85E-04	PKA-reg (cAMP-dependent), Calmodulin, PLC-beta, PKC-alpha, MyHC, MLCK, MRLC, ACM3
23	DNA damage_Mismatch repair	4.68E-04	MutSalpha complex, EXO1, MSH2, HMGB1, MSH6, DNA-PK
24	dCTP/dUTP metabolism	5.73E-04	dUTPase (DUT), POLA2, POLA1, POLE2, RRM2, TK1, Small RR subunit, RRM1, Ribonucleotide reductase
25	Bipolar Disorder	6.99E-04	Ankyrin-G, cPKC (conventional), PKA-reg (cAMP-dependent), Calmodulin, PKC, PLC-beta, PAR4, PKC-alpha, ACM3

Statistical significance was set to $P < 0.05$.

Supplementary Table 4. Top 25 upregulated pathways in the MetaCore analysis of potential maps when comparing JTC-801 treated-MDA-MB-231 cells with the control group

Rank	Maps	*P* value	Network objects from active data
1	IL-1 signaling in melanoma	4.70E-14	COX-2 (PTGS2), IL-1RI, GRO-2, IL-1 beta, IL-6, AP-1, JNK(MAPK8-10), IL-1 alpha, GRO-1, NF-kB, p21, ICAM1, SOD2, MMP-1, IL-8, GRO-3, MMP-9
2	Immune response_IL-1 signaling pathwayF	1.69E-13	COX-2 (PTGS2), IL-1RI, IL-1 beta, IL-6, Sequestosome 1 (p62), EGR1, c-IAP2, AP-1, JNK(MAPK8-10), IL-1 alpha, NF-kB2 (p100), GRO-1, MMP-13, MCPIP, NF-kB, IP10, ICAM1, NF-kB2 (p52), MMP-1, IL-8, MMP-9, GM-CSF
3	Inflammatory mechanisms of pancreatic cancerogenesis	2.34E-13	COX-2 (PTGS2), IL-1RI, IL-32 (NK4), IL-1 beta, IL-6, TNF-R2, EGF, CCL20, AP-1, IL-1 alpha, GRO-1, NF-kB, c-Fos, Angiotensin II, ICAM1, IL-8, MMP-9, G-protein alpha-i family, ENA-78, MMP-2
4	Glomerular injury in Lupus Nephritis	1.80E-11	C5aR, GRO-2, IL-1 beta, IL-6, JNK(MAPK8-10), GRO-1, PDGF-B, NF-kB, IP10, ICAM1, MDA-5, MIP-1-alpha, C3a, MMP-1, IL-8, NGAL, GRO-3, A20, MMP-9, GM-CSF, IFI56
5	Immune response_IL-17 signaling pathways	3.82E-11	COX-2 (PTGS2), IL-1 beta, IL-6, CCL20, GRO-1, NF-kB, c-Fos, GCP2, ICAM1, G-CSF, MMP-1, Stromelysin-1, IL-8, NGAL, MMP-9, GM-CSF, ENA-78
6	Neutrophil chemotaxis in asthma	3.85E-11	C5aR, GRO-2, VEGFR-1, PTAFR, CCR1, GRO-1, NF-kB, MIP-1-alpha, HSP70, PLGF, IL-8, GRO-3, G-protein alpha-i family, ENA-78
7	Role of fibroblasts in the sensitization phase of allergic contact dermatitis	9.01E-11	IL-1RI, IL-1 beta, IL-6, AP-1, IL-1 alpha, NF-kB, Collagen IV, IL-8, MMP-9, MMP-2, Collagen III
8	TNF-alpha and IL-1 beta-mediated regulation of contraction and secretion of inflammatory factors in normal and asthmatic airway smooth muscle	1.55E-10	COX-2 (PTGS2), IL-1RI, GRO-2, IL-1 beta, IL-6, JNK(MAPK8-10), GRO-1, JNK3(MAPK10), NF-kB, Histone H3, c-Fos, PLA2, IL-8, GRO-3, MMP-9, GM-CSF, Histone H4
9	Interleukins-induced inflammatory response in asthmatic airway fibroblasts	1.73E-10	COX-2 (PTGS2), IL-1RI, GRO-2, IL-1 beta, IL-6, IL-1 alpha, GRO-1, NF-kB, c-Fos, ICAM1, G-CSF, IL-8, GM-CSF
10	Release of pro-inflammatory factors and proteases by alveolar macrophages in asthma	3.72E-10	GRO-2, IL-1 beta, IL-6, CXCL16, GRO-1, NF-kB, IP10, MIP-1-alpha, MMP-1, Stromelysin-1, IL-8, MMP-9, GM-CSF, IRF5
11	Transcription_HIF-1 targets	1.84E-09	ID2, Heme oxygenase 1, NOXA, VEGFR-1, WT1, Ceruloplasmin, GLUT3, Angiopoietin 2, PDGF-B, Lysyl oxidase, Transferrin, p21, DEC1 (Stra13), PLGF, ALDOC, MMP-9, Stanniocalcin 2, REDD1, MMP-2
12	Release of pro-inflammatory mediators and elastolytic enzymes by alveolar macrophages in COPD	2.23E-09	IL-1 beta, IL-6, Matrilysin (MMP-7), IP10, MIP-1-alpha, MMP-1, Cathepsin S, IL-8, MMP-9, GM-CSF, MMP-2
13	COVID-19 associated coagulopathy	3.21E-08	C5aR, GRO-2, IL-6, NF-kB, Histone H3, C3a, C3, IL-8, cPLA2, GRO-3, C3b, C3aR, Cathepsin D
14	NF-kB-, AP-1- and MAPKs-mediated proinflammatory cytokine production by eosinophils in asthma	3.61E-08	IL-1 beta, IL-6, CCL22, AP-1, JNK(MAPK8-10), GRO-1, NF-kB, Tryptase, MIP-1-alpha, IL-8, GM-CSF, ENA-78
15	Immune response_IL-6-induced acute-phase response in hepatocytes	4.76E-08	IL-6, Heme oxygenase 1, Hemopexin, Angiotensinogen, GRO-1, SAA1, SAA2, c-Fos, C3, G6PT, Fibrinogen beta
16	Immune response_IL-18 signaling	6.28E-08	COX-2 (PTGS2), IL-1 beta, IL-6, IL-18R1, AP-1, JNK(MAPK8-10), IL-1 alpha, CXCL16, NF-kB, p67-phox, c-Fos, ICAM1, IL-8, MMP-9
17	Eosinophil chemotaxis in asthma	7.77E-08	C5aR, Eotaxin-3, S1P1 receptor, VEGFR-1, PTAFR, CCL20, CCR1, IP10, MIP-1-alpha, C3a, IL-8, G-protein alpha-i family, GM-CSF, C3aR
18	The complement system and macrophages in neuropathic pain	8.69E-08	COX-2 (PTGS2), IL-1RI, C5aR, IL-1 beta, IL-6, C7, TNF-R2, CCR1, GRO-1, NF-kB, Angiotensin II, MIP-1-alpha, C3a, C3, C3b, G-protein alpha-i family, C3aR, Kappa-type opioid receptor, H-Ficolin
19	Signal transduction_PDGF signaling via MAPK cascades	9.57E-08	COX-2 (PTGS2), IL-6, EGR1, Osteopontin, AP-1, JNK(MAPK8-10), MMP-13, PDGF-B, TRPC6, c-Fos, p21, Stromelysin-1, MMP-9, MMP-2
20	Immune response_Histamine H1 receptor signaling in immune response	1.07E-07	IL-6, JNK(MAPK8-10), MMP-13, c-Fos, ICAM1, MMP-1, Stromelysin-1, IL-8, cPLA2, MMP-9, GM-CSF, NF-AT2(NFATC1)
21	IFN-gamma and Th2 cytokines-induced inflammatory signaling in normal and asthmatic airway epithelium	1.60E-07	IL-2R gamma chain, IL-6, Eotaxin-3, IL13RA2, JNK(MAPK8-10), CXCL16, NF-kB, IP10, ICAM1, I-TAC, IL-8
22	Immune response_Lysophosphatidic acid signaling via NF-kB	3.57E-07	COX-2 (PTGS2), IL-6, Angiogenin, CCL20, JNK(MAPK8-10), NF-kB, ICAM1, IL-8, GRO-3, A20, MMP-9, MMP-2
23	Immune response_IL-10 signaling pathway	3.84E-07	ALOX5AP, COX-2 (PTGS2), IL-1 beta, IL-6, Heme oxygenase 1, Fc gamma RII beta, IL-1 alpha, NF-kB, ICAM1, G-CSF, IL-8, MMP-9, GM-CSF
24	Th2 cytokine- and TNF-alpha-induced inflammatory response in asthmatic airway fibroblasts	3.98E-07	COX-2 (PTGS2), IL-6, Eotaxin-3, JNK(MAPK8-10), NF-kB, c-Fos, ICAM1, G-CSF, IL-8, GM-CSF
25	Proinflammatory cytokine production by Th17 cells in asthma	4.46E-07	COX-2 (PTGS2), IL-1RI, C5aR, IL-1 beta, IL-6, CCL20, JNK(MAPK8-10), NF-kB, C3a, C3, IL-8, C3aR

Statistical significance was set to $P < 0.05$.

Supplementary Table 5. Top 25 upregulated pathways in the MetaCore analysis of potential maps when comparing sodium oxamate-treated MDA-MB-231 cells with the control group

Rank	Maps	*P* value	Network objects from active data
1	COVID-19 associated coagulopathy	4.31E-07	IL-6, von Willebrand factor, NF-kB, Histone H3, Tissue factor, C3a, C3, IL-8, cPLA2, C3b, C3aR, Cathepsin D
2	Protein folding and maturation_Angiotensin system maturation	1.74E-06	Angiotensin III, Angiotensin (2-10), Renin, Angiotensinogen, Angiotensin IV, Angiotensin I, Myeloblastin, Angiotensin II, Angiotensin (1-7), Angiotensin (1-9), Cathepsin D
3	Aminoglycoside- and cisplatin-induced hair cell death	6.77E-06	IL-6, NOL3, JNK(MAPK8-10), RelA (p65 NF-kB subunit), FasL(TNFSF6), NF-kB, iNOS, CX3CL1, p67-phox, Histone H3, NOX4, Caspase-1, Histone H2A, Histone H2B, Cathepsin D, Histone H4
4	HDL dyslipidemia in type 2 diabetes and metabolic syndrome X	1.15E-05	Pre beta-1 HDL, S1P1 receptor, APOA1, LIPC (HL), APOE, LIPE, HDL, ABCG1, Nascent HDL
5	Transport_HDL-mediated reverse cholesterol transport	2.75E-05	Pre beta-1 HDL, APOA1, LIPC (HL), APOE, LIPE, HDL, ABCG1, Nascent HDL, Large apoE-rich HDL
6	Immune response_Histamine H1 receptor signaling in immune response	7.06E-05	IL-6, JNK(MAPK8-10), RelA (p65 NF-kB subunit), iNOS, Tissue factor, Stromelysin-1, IL-8, cPLA2, IP3 receptor
7	Glucocorticoids-mediated inhibition of pro-constrictory and pro-inflammatory signaling in airway smooth muscle cells	9.93E-05	IL-6, JNK(MAPK8-10), PGES, RelA (p65 NF-kB subunit), NF-kB, PLA2, Neurokinin-2 receptor, Histone H4, MKP-1
8	Angiogenesis in HCC	1.17E-04	Angiopoietin 1, VEGFR-1, FGF2, PGES, NF-kB, IL-8, Epo, Ephrin-B receptors, IGF-2
9	Colorectal cancer (general schema)	1.23E-04	IL-6, DLL1, EGF, PTCH1, IL-8, WNT, Ephrin-B receptors
10	Vascular endothelial cell damage in SLE	1.48E-04	IL-6, JNK(MAPK8-10), von Willebrand factor, RelA (p65 NF-kB subunit), NF-kB, iNOS, Tissue factor, Caspase-1, C3a, IL-8
11	Role of fibroblasts in the sensitization phase of allergic contact dermatitis	1.50E-04	IL-6, E-cadherin, NF-kB, Collagen IV, IL-8, Collagen III
12	Maturation and migration of dendritic cells in skin sensitization	1.55E-04	IL-6, E-cadherin, HLA-DRB1, JNK(MAPK8-10), NF-kB, MHC class II beta chain, HLA-DRB, IL-8
13	Apoptosis and survival_Granzyme A signaling	1.55E-04	IL-6, Histone H3, Collagen IV, TLR9, HSP70, IL-8, Histone H2B, Histone H4
14	Chemotaxis_CCR1 signaling	1.86E-04	IL-6, NF-kB, IL-8, cPLA2, G-protein alpha-14, G-protein alpha-i family, G-protein alpha-o, IP3 receptor, CCL16
15	The role of KEAP1/NRF2 pathway in skin sensitization	1.90E-04	Heme oxygenase 1, E-cadherin, JNK(MAPK8-10), NF-kB, HSP70, Caspase-1, IL-8
16	Stem cells_Aberrant Hedgehog signaling in medulloblastoma stem cells	1.92E-04	SFRP1, PTCH1, PTCH2, IGF-2, KCTD11
17	TNF-alpha and IL-1 beta-mediated regulation of contraction and secretion of inflammatory factors in normal and asthmatic airway smooth muscle	1.94E-04	IL-6, JNK(MAPK8-10), PGES, RelA (p65 NF-kB subunit), JNK3(MAPK10), NF-kB, Histone H3, PLA2, IL-8, Histone H4
18	Signal transduction_Angiotensin II/AGTR1 signaling via Notch, Beta-catenin and NF-kB pathways	2.08E-04	IL-6, NOTCH3(NEXT), E-cadherin, NOTCH3 (3ICD), Angiotensinogen, RelA (p65 NF-kB subunit), NF-kB, TRPC6, Angiotensin II, IL-8, NOTCH3 receptor
19	The complement system and macrophages in neuropathic pain	2.17E-04	IL-6, NF-kB, iNOS, TLR9, Angiotensin II, PGE2R3, C3a, C3, C3b, G-protein alpha-i family, Substance P receptor, C3aR, Kappa-type opioid receptor, IP3 receptor
20	Immune response_T cell co-signaling receptors, schema	2.50E-04	DNAM1, PP2135, DPP4, TL1A(TNFSF15), BY55, BTLA, CD48, Galectin-9, Collagen III
21	Hedgehog signaling in breast cancer	2.52E-04	E-cadherin, Osteopontin, DHH, Ihh, PTCH1, MDR1
22	Immune response_IL-6-induced acute-phase response in hepatocytes	4.11E-04	IL-6, Heme oxygenase 1, Angiotensinogen, SAA1, SAA2, C3, Fibrinogen beta
23	Regulation of angiogenesis in prostate cancer	4.16E-04	Angiopoietin 1, VEGFR-1, EGF, VEGF-D, PGES, Collagen IV, Angiotensin II, IL-8
24	Demyelination in multiple sclerosis	5.58E-04	PADI2, JNK(MAPK8-10), JNK3(MAPK10), FasL(TNFSF6), iNOS, Apo-2L(TNFSF10), Stromelysin-1, Cathepsin D
25	Neutrophil chemotaxis in asthma	5.81E-04	VEGFR-1, NF-kB, HSP70, IL-8, G-protein alpha-i family, Substance P receptor, Tissue kallikreins

Statistical significance was set to $P < 0.05$.

Supplementary Table 6. Top 25 upregulated pathways in the MetaCore analysis of potential maps when comparing JTC-801/sodium oxamate-cotreated MDA-MB-231 cells with the control group

Rank	Maps	*P* value	Network objects from active data
1	Immune response_Alternative complement pathway	9.83E-10	C5aR, CR1, C9, iC3b, C3dg, Factor B, CD21, C3a, C3, C5 convertase (C3b2Bb), Factor Ba, C3b, Factor Bb, C3 convertase (C3bBb), C3c, Clusterin
2	IL-1 signaling in melanoma	2.58E-09	COX-2 (PTGS2), IL-1RI, GRO-2, IL-1 beta, IL-6, I-kB, AP-1, IL-1 alpha, GRO-1, p21, SOD2, MMP-1, IL-8, GRO-3
3	Immune response_Lectin induced complement pathway	3.64E-09	C5aR, C2, CR1, C9, iC3b, MASP1, C3dg, CD21, C2b, C3a, C3, C3b, C2a, C3c, Clusterin
4	Immune response_IL-1 signaling pathway	3.76E-09	COX-2 (PTGS2), IL-1RI, IL-1 beta, IL-6, Sequestosome 1(p62), I-kB, EGR1, c-IAP2, AP-1, IL-1 alpha, PGES, GRO-1, MMP-13, MCPIP, IP10, MMP-1, IL-8, ZFP36(Tristetraprolin), GM-CSF
5	Immune response_IL-17 signaling pathways	7.34E-09	COX-2 (PTGS2), IL-1 beta, IL-6, I-kB, CCL20, GRO-1, c-Fos, GCP2, G-CSF, MMP-1, Stromelysin-1, C/EBP-beta, IL-8, NGAL, GM-CSF, ENA-78
6	Immune response_Classical complement pathway	8.88E-09	C5aR, C2, CR1, C9, iC3b, C3dg, CD21, C2b, C3a, C3, C3b, C1s, C2a, C3c, Clusterin
7	The complement system and macrophages in neuropathic pain	1.97E-08	COX-2 (PTGS2), IL-1RI, C5aR, C2, IL-1 beta, IL-6, PGE2R4, TNF-R2, GRO-1, C9, Factor B, TLR9, MIP-1-alpha, PGE2R3, C3a, C3, C5 convertase (C3b2Bb), C3b, Factor Bb, C3 convertase (C3bBb), Kappa-type opioid receptor, C2a
8	Interleukins-induced inflammatory response in asthmatic airway fibroblasts	2.50E-08	COX-2 (PTGS2), IL-1RI, GRO-2, IL-1 beta, IL-6, IL-1 alpha, GRO-1, c-Fos, G-CSF, IL-8, GM-CSF, IL-11
9	Neutrophil chemotaxis in asthma	7.16E-08	BDKRB1, C5aR, GRO-2, VEGFR-1, GRO-1, MIP-1-alpha, HSP70, PI3K reg class IB (p101), IL-8, GRO-3, Tissue kallikreins, ENA-78
10	Th17 cells in CF	9.49E-08	IL-1RI, IL-1 beta, IL-6, CFTR, CCL20, GRO-1, IL-21 receptor, GCP2, ROR-alpha, IRF4, G-CSF, IL-8, GM-CSF, MD-2
11	TNF-alpha and IL-1 beta-mediated regulation of contraction and secretion of inflammatory factors in normal and asthmatic airway smooth muscle	1.77E-07	COX-2 (PTGS2), IL-1RI, GRO-2, IL-1 beta, IL-6, PGES, GRO-1, Histone H3, c-Fos, PLA2, IL-8, GRO-3, GM-CSF, NFKBIA, Histone H4
12	Apoptosis and survival_Granzyme A signaling	1.84E-07	IL-1 beta, IL-6, GSDML, Histone H3, Collagen IV, TLR9, HSP70, hnRNP C, IL-8, Granzyme A, Histone H2B, Histone H4
13	IL-17 and IL-17F-induced inflammatory signaling in normal and asthmatic airway epithelium	2.41E-07	IL-6, I-kB, GRO-1, IP10, GCP2, G-CSF, IL-8, GM-CSF, IL-11, ENA-78
14	Inflammatory mechanisms of pancreatic cancerogenesis	2.70E-07	COX-2 (PTGS2), IL-1RI, IL-1 beta, C/EBP, IL-6, Mucin 4, TNF-R2, CCL20, AP-1, IL-1 alpha, GRO-1, c-Fos, IL-8, NFKBIA, ENA-78
15	Release of pro-inflammatory factors and proteases by alveolar macrophages in asthma	4.33E-07	GRO-2, IL-1 beta, IL-6, CXCL16, GRO-1, IP10, MIP-1-alpha, MMP-1, Stromelysin-1, IL-8, GM-CSF, TIMP1
16	Transcription_Role of AP-1 in regulation of cellular metabolism	6.81E-07	FXYD2, AP-1, FasL(TNFSF6), Alpha1-globin, FosB/JunB, c-Fos, p21, JunB, TSG-6, CGB3, Prolactin
17	Alternative complement cascade disruption in age-related macular degeneration	7.19E-07	C5aR, iC3b, Factor B, C3a, C3, C5 convertase (C3b2Bb), Factor Ba, C3b, Factor Bb, C3 convertase (C3bBb)
18	Glomerular injury in Lupus Nephritis	8.15E-07	C5aR, GRO-2, IL-1 beta, IL-6, GRO-1, FasL(TNFSF6), IP10, MDA-5, MIP-1-alpha, C3a, MMP-1, IL-8, NGAL, GRO-3, A20, GM-CSF, IFI56
19	NF-kB-, AP-1- and MAPKs-mediated proinflammatory cytokine production by eosinophils in asthma	2.64E-06	IL-1 beta, IL-6, ST2(L), CCL22, AP-1, GRO-1, Tryptase, MIP-1-alpha, IL-8, GM-CSF, ENA-78
20	Release of pro-inflammatory mediators and elastolytic enzymes by alveolar macrophages in COPD	2.71E-06	MMP-12, IL-1 beta, IL-6, IP10, MIP-1-alpha, MMP-1, Cathepsin S, IL-8, GM-CSF
21	Macrophage and dendritic cell phenotype shift in cancer	2.73E-06	COX-2 (PTGS2), IL-1RI, IL-1 beta, IL-6, PGE2R4, I-kB, DLL1, CD137 ligand(TNFSF9), SHP-1, IRE1, IP10, TLR9, ESR1 (nuclear), JMJD3, IRF4, DLL4, GM-CSF
22	Role of fibroblasts in the sensitization phase of allergic contact dermatitis	3.42E-06	IL-1RI, IL-1 beta, IL-6, AP-1, IL-1 alpha, Collagen IV, IL-8, Collagen III
23	Proinflammatory cytokine production by Th17 cells in asthma	3.75E-06	COX-2 (PTGS2), IL-1RI, C5aR, IL-1 beta, IL-6, CCL20, IL-21 receptor, ROR-alpha, IRF4, C3a, C3, IL-8
24	Immune response_Histamine H1 receptor signaling in immune response	6.76E-06	IL-6, I-kB, MMP-13, c-Fos, MMP-1, Stromelysin-1, IL-8, cPLA2, GM-CSF, NF-AT2(NFATC1), NFKBIA
25	Signal transduction_Non-apoptotic FasR(CD95) signaling	7.58E-06	GRO-2, IL-1 beta, IL-6, I-kB, EGR1, AP-1, sFasL, GRO-1, FasL(TNFSF6), c-Fos, SFK, PI3K reg class IB (p101), IL-8, GRO-3, NFKBIA

Statistical significance was set to P < 0.05.

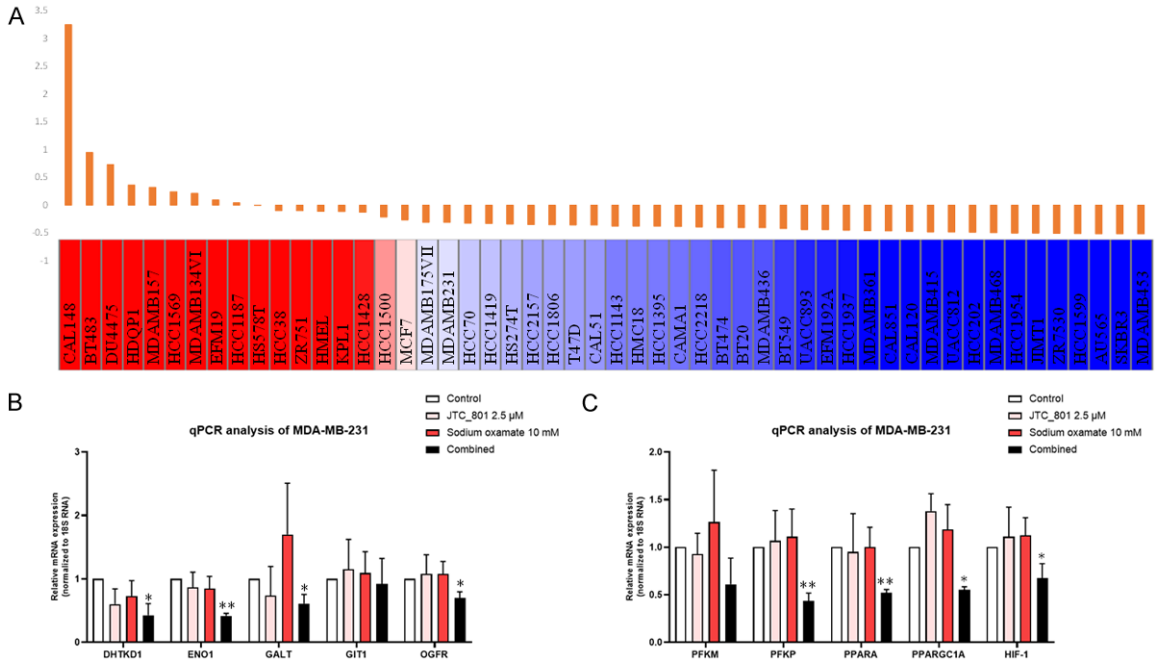

Supplementary Figure 6. OPRL1 expression in breast cancer cell line and validation of bioinformatics data in MDA-MB-231 cells. (A) RNA-Sequencing analysis of OPRL1 mRNA in different breast cancer cell lines in the Cancer Cell Line Encyclopedia (CCLE). Red indicates overexpression (left), while blue indicates downregulation (right) of OPRL1 in each cancer cell line. The RNA was extracted from JTC-801/sodium oxamate-cotreated group in MDA-MB-231 cells, then the (B) opioid receptor- and (C) glycolysis-related genes were further validated via RT-qPCR. $*P < 0.05$; $**P < 0.01$.

JTC-801 and sodium oxamate

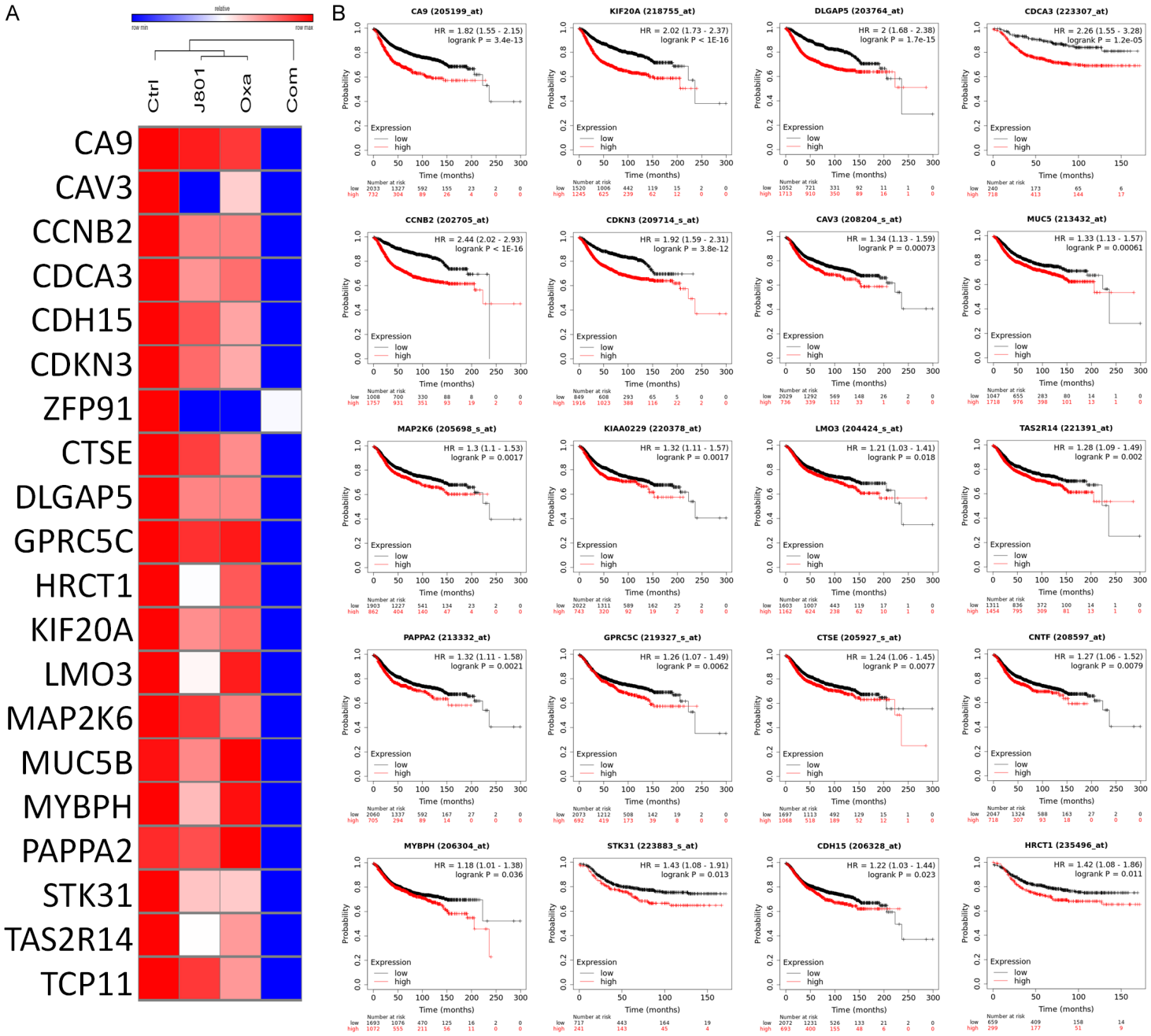

Supplementary Figure 7. Relationships of lower expressions of genes in the JTC-801 plus sodium oxamate co-treatment group with distant metastasis-free survival in breast cancer patients. A. A heatmap represents low-expression genes in the JTC-801/sodium oxamate-cotreated group via RNA-sequencing data of MDA-MB-231 cells. Low-expressed genes in the cotreated group were selected for further study. B. Impacts of the low-expressed genes on distant metastasis-free survival of breast cancer patients were studied using the KM Plot database. Red lines indicate patients with high transcriptional levels, whereas black lines indicate those with low expression levels. Hazard ratios (HRs) with 95% confidence intervals (CIs) and log-rank *p* values are illustrated.